

OPTIMIZATION OF REDUCED BEAM SECTION MOMENT CONNECTIONS

by

Lawal, Morayo Oluwaseun

B.Eng. (Civil Engineering) Covenant University, Nigeria, 2016

A major research paper
presented to Ryerson University

in partial fulfilment of the
requirements for the degree of
Master of Engineering
in the program of civil engineering

Toronto, Ontario, Canada, 2020

©Morayo Lawal 2020

**AUTHOR'S DECLARATION FOR ELECTRONIC SUBMISSION OF A MAJOR
RESEARCH PAPER (MRP)**

I hereby declare that I am the sole author of this major research paper. This is a true copy of the MRP, including any required final revisions.

I authorize Ryerson University to lend this MRP to other institutions or individuals for the purpose of scholarly research.

I further authorize Ryerson University to reproduce this MRP by photocopying or by other means, in total or in part, at the request of other institutions or individuals for the purpose of scholarly research.

I understand that my MRP may be made electronically available to the public.

OPTIMIZATION OF REDUCED BEAM SECTION MOMENT CONNECTIONS

Lawal, Morayo Oluwaseun,

Master of Engineering

Civil Engineering, 2020

ABSTRACT

Reduced beam section (RBS) moment connections also referred to as Dog-bone connections are commonly used in seismic resistant steel moment frames. In RBS connections, the top and bottom flanges of the steel beam are selectively trimmed in the area adjacent to the beam to column connection. This is to ensure that under seismic loading, plastic hinges are formed in the beam not in the column.

The purpose of this study is to optimize the cyclic responses of RBS moment connections including those with sloping beams. Using a response surface method, predictive equations are developed for the response characteristics, such as initial stiffness, plastic strain index, moment capacity, hysteretic energy dissipation, and strength degradation rate. The optimization studies consider objectives leading to higher stiffness, lower plastic strain index, maximum moment capacity, higher hysteresis energy dissipation and lower strength degradation. The optimization results obtained shows that beam slope angle greater than 27.8° will experience fracture, high inelastic demand with higher strength degradation and more intense buckling.

ACKNOWLEDGEMENT

I am grateful to Almighty God, for His guidance, blessing for without His grace this study would not have been possible. My master's study at Ryerson University was a great journey of learning, research and full of motivation. I owe a lot to people who made this journey's achievement a success.

My deepest gratitude and enormous appreciation to my supervisor, Professor Saber Moradi. It was a privilege to work with him, and I learnt a lot from his knowledge and expertise. All meetings we had were helpful and encouraging.

My sincere thanks to Professor Tom Duever for teaching me the design of experiment method which was greatly beneficial in this research.

I would like to appreciate the support and encouragement of my parents, Engr. & Mrs. Adekunle Lawal, my siblings and friends in the course of my study.

Table of contents

AUTHOR'S DECLARATION	ii
ABSTRACT	iii
ACKNOWLEDGEMENT	iv
LIST OF TABLES	viii
LIST OF FIGURES	ix
LIST OF APPENDICES	xi
1 INTRODUCTION	1
1.1 General.....	1
1.2 Scope and objectives.....	2
2 LITERATURE REVIEW: REDUCED BEAM SECTION (RBS) MOMENT CONNECTIONS	3
2.1 RBS.....	3
2.2 RBS with connection flexibility.....	4
2.3 RBS radius cut subjected to cyclic loading.....	5
2.4 Effect of web stiffener.....	5
2.5 RBS with deep wide flange columns.....	6
2.6 Weak axis RBS connection.....	7
2.7 Shape optimization of reduced beam section under cyclic loads.....	7
2.8 Retrofit methods with RBS.....	8
2.9 Non-orthogonal RBS moment connections.....	9
2.10 The effect of different parameters on non-orthogonal RBS moment connections.....	9
2.10.1 <i>Effects of design factors on the cyclic response of sloped RBS moment connections</i>	9
2.10.2 <i>Column axial load effects on skewed SMF RBS connections</i>	10
2.10.3 <i>Beam slope effects on sloped RBS moment connections at roof floor</i>	10
2.10.4 <i>Slope angle effect</i>	10
2.11 Evaluation of sloped RBS moment connections.....	10
3 THE USE OF RESPONSE SURFACE METHOD (RSM) IN EARTHQUAKE ENGINEERING AND SEISMIC DESIGN	12
3.1 Response surface analysis and optimization of controlled rocking steel braced frames (CRSBFs).....	12
3.2 Predictive equations for PT steel beam-column connections using RSM.....	12
3.3 RSM used in seismic fragility analysis of existing building frame.....	12

3.4	Application of RSM in seismic performance reliability of reinforced concrete (RC) structures.....	13
3.5	Use of RSM to generate system level fragilities for existing curved steel bridges...	13
3.6	An application of the RSM in building seismic fragility estimation.....	14
3.7	Probabilistic nonlinear analysis of concrete-faced rock fill (CFR) dams by Monte Carlo simulation (MCS) using RSM	14
3.8	RSM with random factors for seismic fragility of reinforced concrete frames	14
3.9	Summary	15
4	PREDICTIVE EQUATIONS FOR RBS MOMENT CONNECTIONS	16
4.1	General	16
4.2	Response surface methodology (RSM).....	16
4.3	Factors and response variables.....	17
4.4	Results and response surface metamodels	18
4.4.1	<i>Initial stiffness (K_i)</i>	<i>20</i>
4.4.2	<i>Equivalent Plastic Strain Index (PI)</i>	<i>21</i>
4.4.3	<i>Moment capacity (M_{max})</i>	<i>22</i>
4.4.4	<i>Hysteretic energy dissipation (HED).....</i>	<i>23</i>
4.4.5	<i>Strength degradation rate (SDR)</i>	<i>23</i>
5	MULTIPLE RESPONSE OPTIMIZATION	25
5.1	General	25
5.2	Desirability function for multiple response optimization.	25
5.3	Optimization objectives.....	26
5.4	Results and discussions	30
5.4.1	<i>Results of the first optimization analysis</i>	<i>30</i>
5.4.2	<i>Results of the second optimization analysis</i>	<i>32</i>
5.4.3	<i>Results of the third optimization analysis</i>	<i>35</i>
5.4.4	<i>Results of the fourth optimization analysis</i>	<i>38</i>
5.4.5	<i>Results of the fifth optimization analysis</i>	<i>41</i>
5.4.6	<i>Results of the sixth optimization analysis</i>	<i>44</i>
6	SUMMARY AND CONCLUSION	47
6.1	Summary	47
6.2	Conclusion.....	47
6.2.1	<i>Predictive equations.....</i>	<i>47</i>
6.2.2	<i>Optimization of sloped RBS connection.....</i>	<i>48</i>
	APPENDICES	520

REFERENCES52

LIST OF TABLES

Table 4.1. Factors considered in this study.....	17
Table 4.2. Factors combination.....	18
Table 4.3. Response values.....	19
Table 5.1. Objectives and constraints for the first optimization problem.....	27
Table 5.2. Objectives and constraints for the second optimization problem.....	28
Table 5.3. Objectives and constraints for the third optimization problem.....	28
Table 5.4. Objectives and constraints for the fourth optimization problem.....	29
Table 5.5. Objectives and constraints for the fifth optimization problem.....	29
Table 5.6. Objectives and constraints for the sixth optimization problem.....	29
Table 5.7. Responses with their desirability.....	30
Table 5.8. Responses with their desirability.....	33
Table 5.9. Responses with their desirability.....	36

LIST OF FIGURES

Figure 2.1. Various types of RBS cuts a) tapered cut, (b) radius cut, (c) straight cut.....	3
Figure 2.2. Stress profile across beam flange (a) strong-axis connection (b) weak-axis connection.....	7
Figure 2.3. Connection retrofitted method (a) RBS only (b) RBS reinforced by bottom flange reinforcement (c) RSR shaped bottom flange reinforcement.....	8
Figure 4.1. Variation of initial stiffness response variable to different factors.....	21
Figure 4.2. Variation of plastic strain index with respect to different factors.....	21
Figure 4.3. Variation of moment capacity with respect to different factors.....	22
Figure 4.4. Variation of hysteretic energy dissipation with respect to different factors.....	23
Figure 4.5. Variation of strength degradation with respect to beam slope angle and beam web slenderness ratio.....	24
Figure 5.1. The desirability function when the optimization goal is to: (a) maximize the response; (b) minimize the response; (c) assign a target for the response.....	26
Figure 5.2. First optimization analysis, the desirability function at the optimum condition versus: (a) beam web slenderness ratio; (b) beam flange slenderness ratio; (c) slope angle; (d) RBS depth to beam flange width ratio; (e) column flange slenderness ratio	31
Figure 5.3. Contour plot of desirability at the optimum condition: (a) beam slope versus beam web slenderness ratio; (b) beam slope versus beam flange slenderness ratio; (c) beam slope versus RBS depth to beam flange width ratio; (d) beam slope versus column flange slenderness ratio.....	32
Figure 5.4. Second optimization analysis, the desirability function at the optimum condition versus: (a) beam web slenderness ratio; (b) beam flange slenderness ratio, (c) slope angle; (d) RBS depth to beam flange width ratio; (e) column flange slenderness ratio.....	34
Figure 5.5. Contour plot of desirability at the optimum condition: (a) beam slope versus beam flange slenderness ratio; (b) RBS depth to beam flange width ratio versus beam slope; (c) beam slope versus beam web slenderness ratio.....	35
Figure 5.6. Third optimization analysis, the desirability function at the optimum condition versus: (a) beam web slenderness ratio; (b) beam flange slenderness ratio, (c) slope angle; (d) RBS depth to beam flange width ratio; (e) column flange slenderness ratio.....	37
Figure 5.7. Contours plots of the desirability functions for different factors.....	38

Figure 5.8. Fourth optimization analysis, the desirability function at the optimum condition versus: (a) beam web slenderness ratio; (b) beam flange slenderness ratio, (c) slope angle; (d) RBS depth to beam flange width ratio; (e) column flange slenderness ratio.....40

Figure 5.9. Contours plots of the desirability functions for different factors.....41

Figure 5.10. Fifth optimization analysis, the desirability function at the optimum condition versus: (a) beam web slenderness ratio; (b) beam flange slenderness ratio, (c) slope angle; (d) RBS depth to beam flange width ratio; (e) column flange slenderness ratio.....43

Figure 5.11. Contours plots of the desirability functions for different factors.....44

Figure 5.12. Sixth optimization analysis, the desirability function at the optimum condition versus: (a) beam web slenderness ratio; (b) beam flange slenderness ratio, (c) slope angle; (d) RBS depth to beam flange width ratio; (e) column flange slenderness ratio.....45

Figure 5.13. Contours plots of the desirability functions for different factors.....46

LIST OF APPENDICES

Figure A1. Variation of initial stiffness response variable to different factors.....	50
Figure A2. Variation of plastic strain index with respect to different factors.....	50
Figure A3. Variation of moment capacity with respect to different factors.....	51
Figure A4. Variation of hysteretic energy dissipation with respect to different factors.....	51

CHAPTER 1

1 INTRODUCTION

1.1 General

The aftermath of the earthquakes that occurred in Northridge, Los Angeles 1994 and Kobe, Japan 1995, structural engineers discovered connection fracture in about 60% of the inspected 155 steel moment frame building (Lignos et al. 2010). The connection fracture that occurred was reported as some of them started at the bottom flange weld and spread to the column flange and the beam web (Aswad et al. 2019).

During the earthquake, it was observed that no steel collapsed except for brittle failure modes in the steel connection, this made structural engineers reconsider the design, detailing and construction of steel moment resisting frames (Lignos et al. 2010). In order to enhance the moment resisting frames, the following methods were proposed:

- Reinforcing the connections and weakening the beam in region of the connection
- Formation of plastic hinges outside the connection leading to a reduction in force and moment at that region (Roudsari et al. 2015; Oh et al. 2007).

This idea was first proposed and tested by Plumier in 1990 which is now called reduced beam section (dog-bone connections). In RBS moment connection, the beam flanges are selectively trimmed in the regions adjacent to the beam to column connection with the different shape of the cut-offs which are constant cut, tapered cut, radius cut and others. Using RBS makes yielding and plastic hinge formation to occur within the reduced section of the beam and it restricts moment that can be developed at the face of the column (Jones et al. 2002).

The smaller moments generated at the face of the column for RBS connection makes it advantageous in a strong column weak beam requirement, minimizing column double plate requirements and it is relatively easy to construct. Despite the major advantages of RBS, there are also disadvantages of RBS moment connection such as slight structural lateral strength and stiffness decrease, increased possibility of local buckling on web, lateral torsional buckling increased on the stress region of the reduced beam section (Engelhardt, 1999).

Modern architectural design requires the use of non-orthogonal connections such as sloped and skewed connections. The adverse effects of the beam slope angle on the connection performance have been identified by previous research studies such as high strain demands at the heel location and brittle fracture at the location of weld access hole, fracture at beam flange

welds. The effect of beam slope angle in conjunction with other potentially important factors on the behaviour of RBS connections has not been studied yet. In order to understand the effect of all parameters and their potential interactions, statistical analysis would need to be performed.

1.2 Scope and objectives

The objective of this study is to understand the factors affecting non-orthogonal RBS moment connection under seismic loading, developing predictive equations for the response characteristics and optimise the performance of orthogonal and non-orthogonal RBS moment connection. A sensitivity study has been reported in a previous research Mohammadi Nia & Moradi, (2020) on evaluation of beam slope angle along with different design factors on the cyclic response of RBS moment connections. This research develops predictive equations, optimization for the response characteristics of non-orthogonal RBS moment connection and identifies region i.e. factor combinations where optimum conditions are achieved in order to improve response characteristics. The optimization objective is to maximise the response characteristics including initial stiffness, moment capacity, hysteretic energy dissipation, and strength degradation rate and minimise plasticity index.

CHAPTER 2

2 LITERATURE REVIEW: REDUCED BEAM SECTION (RBS) MOMENT CONNECTIONS

2.1 RBS

In Jin & El-Tawil (2005), research studies were conducted to understand the behaviour of RBS connections. From the experimental testing, three types of RBS moment connection were evaluated such as tapered cut, radius cut and straight cut. RBS showed lateral torsional buckling in the beam which led to beam strength deterioration and it was observed that the use of composite slab with reduced beam had no adverse effect on the performance rather it improved the behaviour of the RBC connection by providing additional bracing to the beam. The overall cyclic connections observed during the experiment shows that RBS performed well for the use in special moment resisting frames while tapered cut and radius cut showed better performance than constant cut.

The numerical simulation carried out with the aid of software helped to support results from the experimental testing. The analyses performed showed that using a tapered cut RBS connection can help to concentrate the beam rotation at lower strain demand, but it could develop uniform plastic strains in the reduced flange region. A radius cut was able to lessen the strain concentration in the critical region compared to non-RBS connection.

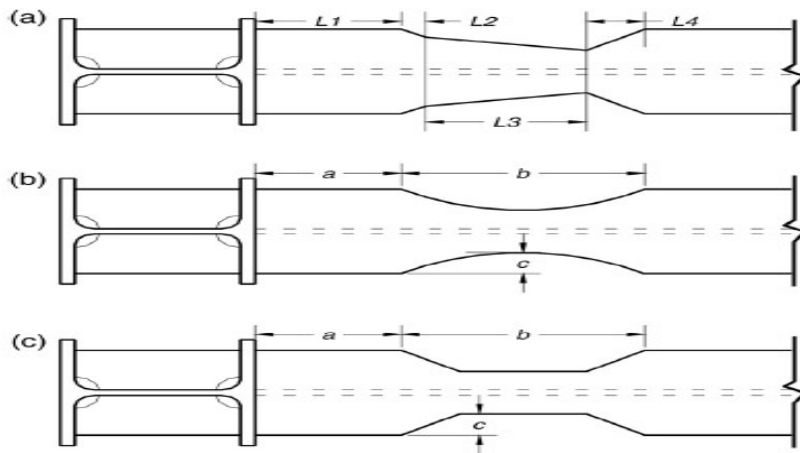


Figure 2.1. Various types of RBS cuts a) tapered cut; (b) radius cut; (c) straight cut. Adapted from “Seismic performance of steel frames with reduced beam section connections” by J. Jin and S. El-Tawil, 2005, *Journal of Constructional Steel Research*, 61(4), 453–471. Copyright 2004 by Elsevier Ltd.

2.2 RBS with connection flexibility

A numerical study by Ghassemieh & Kiani, (2013) was conducted on the seismic response of a building frame using RBS connection. Three building frames with 4, 8 and 16 stories were used with respect to semi-rigid and fully rigid connections. A nonlinear static pushover and dynamic analysis was performed in which the results were compared in terms of inter-story drifts, total drifts, story shears and shear deformation in panel zone. Two methods were proposed to evaluate the micro behaviour of the structural model

- Centre to centre line dimension of beams and columns
- Panel zone deformation and exact length of beams and columns

The first one is the most used in structural analysis, but it is not a good and effective method for the performance as a significant portion of the total storey drift of moment resisting frames is occur in the panel zone region of beam to column joint. The stiffness of the beam-to-column connections were calculated in order to determine the flexibility of the beam-to-column connection. The results from the micro behaviour show that RBS connection does not act completely rigid. Stiffness parameter was used to determine the degree of rigidity of the connection and the acquired stiffness parameters for connection are between 8 and 10, which is smaller than the required value >20 for fully rigid connection suggested by AISC. Thus, the connection flexibility of the beam-to-column to be considered in conventional design methods, and therefore, it is compulsory to include the connection elements as part of the analysis of the structural system.

The results from the static pushover analysis shows that the initial stiffness and over strength factors of the RBS frames with flexibly connected frames are less than RBS frames with semi rigid connections. The $P-\Delta$ effects become more effective for 16-story frames under LA30 earthquake ground motion. The four- and eight-story frames experience higher inter-story drift in the upper stories with flexible beam-to-column connections in comparison with simulation based on fully rigid connections. The influence of connection flexibility on the seismic performance of multi-story frame structures seems to be critical when the $P-\Delta$ effects become very effective in 16-story frame. The nonlinear dynamic analysis showed that analysis of RBS frames, integrating the flexibility of beam-to-column connection in the structural analysis, leads to moment redistribution in beams and results in decreasing the demand in beams and columns. The nonlinear performance of the beam-to-column connection in analysing RBS frames, beam end moments decreased and the flexibility of the beam-to-column connection in analysis of RBS frames reduces the shear demand and shear distortion in the panel zone. The

beam-to-column connection as an element in the structural analysis increased the role of RBS on reducing the seismic demand in the panel zone.

2.3 RBS radius cut subjected to cyclic loading

An experimental study by Pachoumis et al. (2009) was conducted on RBS moment connection with radius cut with respect to the cycling loading. Two specimens were used for this experiment with the idea of combining RBS together with a beam-to-column connection of high-quality welds at the face of the column. Double web plates and continuity plates, with the thickness equal to the beam flange thickness, were used at the column so that they could produce a strong panel zone, forcing the formation of the plastic hinge in the weakening zone. The major difference in the specimen is the radius cut geometrical parameter and a non-linear analysis was used to simulate these specimens.

The analysis was conducted by applying cyclic loading with amplitude displacement at the top of the beam in a distribution of 1m from the face of the column. Several complete loading cycles were applied to each specimen with displacement amplitudes, the displacement expected to yield the specimen. From the results the cyclic performance of the reduced beam section moment connection performed excellent when the plastic hinge is formed at the RBS area and no weld fracture was observed. The first RBS specimen reached over the acceptable plastic rotation without fracture, supporting the overall validity of the design procedure. Trimming the flanges of the beam around the connection let the provided moment capacity be equal to that of the demand value, an enlarged plastic zone can be achieved, and the deformation capacity can be improved. The second RBS specimen showed very poor performance as yielding was observed at the beam's bottom flange near the face of the column and not at the RBS area.

2.4 Effect of web stiffener

A research study by Roudsari et al. (2015) was done to investigate the effects of suitable web stiffeners on preventing the deterioration effect of the hysteresis curve for RBS connections. A nonlinear finite element analyses on different RBS sections with radius cut, straight cut, and drilled-flange RBS connection showed that different web stiffeners considerably contribute to the enhancement of seismic performance of RBS connections. The effects of factors such as the geometry and the number of the stiffeners, the distance between the stiffener and column side, and the length and thickness of the stiffener on the seismic performance of RBS connections were also considered.

In order to study the effect of stiffener on the behaviour of RBS, different horizontal and vertical stiffeners with different lengths, thicknesses, geometries, and quantities were used in

their models. Each model was subjected to cyclic loading up to a rotation of 0.1 radians. Finite element analyses were also performed with the material and geometrical non-linearity's being considered. Different models with the performance of stiffeners were assessed.

RBS connections show reduced hysteresis performance from 0.03 to 0.04 radian rotations. The decrease in the width of beam flange reduces the section's resistance to lateral torsional buckling, and as a result, the possibility of local buckling in the web increases. The geometry of the stiffener (such as its length and angle) influences the performance of connections more than thickness does. The use of vertical and horizontal stiffeners can eliminate the deterioration in the RBS beams made of medium sections up to a rotation of 0.1 radians. The effect of stiffeners on larger sections with radius and straight cuts is considerable and improves the behaviour of such sections. However, compared to the lighter sections, the effect is not as strongly seen. For large sections, the diagonal stiffeners with radius and straight cuts are more suitable.

2.5 RBS with deep wide flange columns

An experimental study by Ricles & Zhang, (2006) was conducted to know the effect of deep wide flange column on the seismic performance of RBS connections. The use of deep column with RBS connection is to control seismic drift and for economic reasons. The study involved both finite element analysis and experimental test using six full scale specimen and the parameters considered were column sizes, beam size, floor slab and supplemental lateral brace at the end of RBS. The specimens were designed in accordance with the procedure by Engelhardt, (1999) for RBS connection thereby the beam design moment at the column face is limited to the expected plastic moment capacity of the beam.

Based on the results derived from the experiment, the composite floor slab used was able to provide restraint to the top flange of the beams thereby reducing the magnitude of beam top and bottom flange lateral movement in the RBS. The reduction in the lateral movement resulted in reducing the torque applied to the column from RBS. Heavier columns with larger torsional stiffness have a reduce column twist while smaller beams sections impose a small torque to a column due to a smaller flange force developed in the beam. Column twist in an RBS connection with a weaker panel zone is reduced due to the reduced amount of local and lateral buckling in the RBS. The specimens having a composite slab with lateral bracing at the RBS met the criteria in Appendix S of the AISC Seismic provisions for qualifying the connection for seismic resistant design.

2.6 Weak axis RBS connection

This study conducted by Gilton & Uang, (2002) is concerned with the cyclic response and design recommendations for weak-axis RBS connections. Accounting for the difference between the stress profile along beam flange in strong and weak axis connections is shown in Figure 2.2, the tests performed included two different specimens (designed, fabricated and constructed with simulated field conditions), which were loaded quasi-statically using standard SAC protocol. FE analytical results were correlated with the experimental results, and significant parameters were addressed, namely the effect of RBS on stress flow, the necessity of far-side continuity plate in the connection configuration, the effect of its trimming and the beam shear stress profile near groove weld. A design procedure was recommended, and based on results the following conclusions drawn were: prevention of brittle weld fracture was achieved in the presence of RBS, which may reduce the strain concentration near the groove weld by a factor of about three; most of yielding and inelastic rotation took place in the vicinity of the RBS, with no contribution of column and panel zone, a continuity plate is not necessary on the far side of the one-sided connection; the beam flange tensile force may be effectively reduced by allowing a continuity plate stick out of at least 76 mm from the column flange tips; if the beam flange width is less than 70% of the width of the continuity plate the corner of the plate should be trimmed and the majority of the beam shear is taken by the beam web.



Figure 2.2. Stress profile across beam flange (a) strong-axis connection (b) weak-axis connection. Adapted from “Cyclic response and design recommendations of weak-axis reduced beam section moment connections” by C.S. Gilton and C. Uang, 2002, *Journal of Structural Engineering Vol.128, Issue 4*. Copyright 2002 by the American Society of Civil Engineers.

2.7 Shape optimization of reduced beam section under cyclic loads

Optimizing the shape of the RBS cut can increase the energy dissipation capacity of the connection, and reduce fracture in the flange. Ohsaki et al. (2009) used a finite element analysis and a simulated annealing program generates new coordinates of the control points to address the optimization problem of the design variables. The main goal is to control the area defined by the vectors which consist of the maximum distance for each variable. Numerical results

were compared to the experimental results and it was observed that optimal shapes can be successfully obtained by simulated annealing in conjunction with a finite element analysis code, the optimal shape also strongly depends on the upper bound of the equivalent plastic strain, which is to be specified in practice based on the performance required for each frame. The energy dissipation capacity can be significantly improved by optimization compared with the normal beam with uniform flange width.

2.8 Retrofit methods with RBS

Effectiveness of different retrofit methods in improving the deformation capacity of existing moment connections in composite beams was investigated by Oh et al. (2007). The three retrofit methods considered are reduced beam section (RBS) only, RBS with bottom flange reinforcement (RBR) and an RBS-shaped bottom flange reinforcement (RSR) as shown in Figure 2.3. Finite element model was conducted to identify causes of the connection failures and the potential for cracking only through the development of stress and strain states that would facilitate fracture. Based on the analytical and test results, the following conclusions are drawn: The use of RBS only did not adequately improve the deformation capacity of the existing moment connection, the retrofitted methods RBR and RSR were able to move the plastic hinge away from the face of the column and also reduce the stress levels in the region of the beam bottom flanges which eventually improved the deformation capacity. It was observed that RBR and RSR were able to achieve more reliable connection performance even in a composite connection.

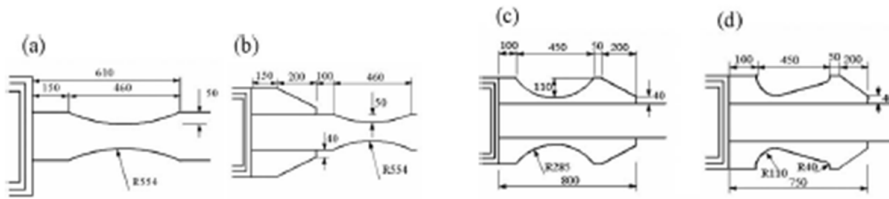


Figure 2.3. Connection retrofitted method (a) RBS only (b) RBS reinforced by bottom flange reinforcement (c & d) RSR shaped bottom flange reinforcement. Adapted from “Cyclic performance of existing moment connections in steel retrofitted with reduced beam section and bottom flange reinforcement” by S. H. Oh, Y. Ju. Kim and T.-S. Moon, 2007, *Canadian Journal of Civil Engineering; Ottawa, 128, Issue 4*. Copyright 2007 by National Research Council Canada.

2.9 Non-orthogonal RBS moment connections

Ball (2011) discusses the structure and the cyclic testing program that was applied to meet the requirements the proposed non-orthogonal RBS connections in accordance with ANSI/AISC 341, for use on the LAX TBIT Modernization Project. Non-orthogonal RBS moment connections were used between beams and columns because some of the beams were sloped and curved. To evaluate the performance of non-orthogonal RBS moment connections, four full-scale specimens were subjected to laboratory testing. Specimens 1 and 2 were simulated such that the moment connection between a sloping curved beams framing into one side of a sloping column, two simulated lateral braces were provided for the beam and one lateral brace was provided for the column. Specimens 3 and 4 simulated two-sided moment connections of sloping straight beams framing into the top end of a vertical column, two lateral braces were provided for the column, and no additional bracing was provided for the beams.

The results from the testing shows that Specimens 1 and 2 had a similar cyclic performance and yielding in the beam flanges was observed at a drift level of 3% for specimen 1 and 2% for specimen 2. Brittle fracture was also observed in both specimens at the beam top flange welded joint during the second cycle at 4% drift for specimen 1 and during the first cycle at 5% drift for specimen 2. Furthermore, specimen 2 relatively showed an enhanced performance than specimen 1 which is due to the deeper RBS cut of specimen 2. Specimens 3 and 4 showed energy dissipation in the form of yielding and buckling in beams, column and panel zone. Lateral–torsional buckling of the beams and twisting of the column at 4% drift occurred in both specimens.

2.10 The effect of different parameters on non-orthogonal RBS moment connections

2.10.1 *Effects of design factors on the cyclic response of sloped RBS moment connections*

Mohammadi Nia & Moradi, (2020) conducted a sensitivity analysis on the effect of thirteen different design parameter on the cyclic response of RBS connections. The cyclic response of RBS connections is evaluated using seven response variables, including initial stiffness, rupture index, plasticity index, moment capacity, yield moment, hysteretic energy dissipation, and strength degradation rate. Design-Expert statistical software was used to generate the factor combinations for a two-level fractional factorial design and to determine significant factors and interaction effects. Beam slope angle and beam web slenderness ratio were the most significant factors influencing the response variables for RBS connections. RBS connections with larger slope angles experience fracture, high strain demands and greater strength degradation.

2.10.2 Column axial load effects on skewed SMF RBS connections

Desrochers et al. (2018) investigates the effects of column axial loads on column twisting and yielding in skewed Special Moment frame RBS connections. The use of finite element software to analyse was used for 48 simulations representing 3 beam-column configurations, 4 levels of beam skew, and 4 levels of column axial load. The results from the analysis showed that when lateral beam-skew is increased and axial force is applied, it has little effect on connection moment capacity in the absence of column local buckling. An increase in column twist is observed due to increased skew angles and increased column depth. Applied column axial loads (up to 25% ΦP_n) in skewed SMF connection geometries have insignificant effect on resulting column twist. The beam-skew angle influences the column flange yielding near the beam-to-column connection and with increased skew angle leading to increased column flange yielding due to distortion induced stresses.

2.10.3 Beam slope effects on sloped RBS moment connections at roof floor

Hong (2019) investigated the effect of beam slope at roof floor on the response of RBS connections with the use of finite element analysis. The finite analysis indicated that plastic hinges were formed in the downward beam, but the upward beams experienced the yielding, only in the bottom portion of the beam at RBS cut location. Irregularity in flexural response occurred at the column tip at a story drift of 0.04 rad when the beam was sloped at angle of 5° and 10°. Force demand in the connection welds of downward beam was always higher at the heel location compared to at the toe location.

2.10.4 Slope angle effect

Mashayekh (2017) evaluated the effect of sloped angle, two RBS specimens with the same beam and columns sizes were tested. The beams were framed into the columns with a 25° angle. The centreline of the RBS section was parallel to the column centreline, while the centre line of the RBS section in Specimen S2 was perpendicular to the beam span. The results obtained from both experimental and analytical studies showed that force demand can be considerably higher at the heel location rather than toe location. A force concentration factor (FCF) was proposed that can show intensity of the force concentration at the heel location. The use of FCF and the proposed truss model can be a systematic method to predict the potential of fracture for any sloped connections.

2.11 Evaluation of sloped RBS moment connections

Kim et al. (2016) evaluated the effects of two sloped (RBS) moment connections with an angle of 28°. A finite element analysis was conducted, and the results obtained are: cyclic testing

showed that both specimens experienced brittle fracture at the top flange, heel location in this configuration, although the connections successfully passed the acceptance criteria of AISC 341 for use in an SMF, the brittle nature of the failure mode was not characteristic of an orthogonal RBS connection where a ductile response was expected. An increase in the depth of the RBS cut can improve the ductile behaviour of sloped connections with heavy W-sections.

CHAPTER 3

3 THE USE OF RESPONSE SURFACE METHOD (RSM) IN EARTHQUAKE ENGINEERING AND SEISMIC DESIGN

3.1 Response surface analysis and optimization of controlled rocking steel braced frames (CRSBFs)

Moradi & Burton, (2018) used sensitivity analyses to determine the factors and active interactions influencing the seismic response of CRSBFs. Six input variables such as gravity load on a rocking column per floor (P_d), initial PT force per strand (F_{pt}), fuse yield stress (σ_{yf}), fuse strain hardening ratio (α_f), fuse modulus of elasticity (E_f), PT strands modulus of elasticity (E_{pf}), were considered in the sensitivity analysis in addition to the variations in earthquake intensity and rocking frame aspect ratio. Three response variables, including peak roof drift (PRD), residual roof drift (RRD), and peak floor horizontal acceleration (PFA) were recorded in each nonlinear response history analysis. From the sensitivity analysis, the influential factors identified are used to perform a multiple response optimization. A response surface models are used to predict the response demand and perform a multiple response optimization. It was observed from the optimization study that optimal conditions for minimizing seismic response demands is to have lower fuse yield stress and initial PT force per strand.

3.2 Predictive equations for PT steel beam-column connections using RSM

Moradi (2016) used RSM in generating predictive equations for PT steel beam-column connection. The response variable of the PT connections includes initial stiffness (K_i), decompression force (F_{deco}), load capacity (F_{max}), decompression drift level (θ_{deco}), and maximum drift level (θ_{max}). The significant factors are post-tensioning force, beam depth, beam flange thickness and width, span length, and height (column length). The Design-Expert software was used to find response surface models using a least-square regression analysis and 32 experiment runs were conducted. Ten additional simulation runs were performed in ANSYS to assess the accuracy of predictions using RSM. The results showed that by comparing the predicted response quantities (using the metamodels) with the corresponding response quantities from simulation or test results, the accuracy of the metamodels was confirmed.

3.3 RSM used in seismic fragility analysis of existing building frame

Sarkar et al. (2015) conducted a numerical analysis on the seismic fragility analysis of an existing building frame. A typical moment resisting 2D concrete frame for the proposed simulation-based approach of Seismic fragility analysis using moving least square method (MLSM) based RSM. For the generation of the RSM, two sampling method was used saturated

design and central composite design (CCD). The input variables used were concrete characteristic strength (F_{ck}), steel yield strength (F_y), structural damping and PGA. The response variables were mean and standard deviation. For the relationship between the input and response variable least square method (LSM) based RSM and moving least square method (MLSM) based RSM was applied. A fragility curves were obtained for three performance levels including Immediate Occupancy (IO), Life Safety (LS), and Collapse Prevention (CP) by all the four response surfaces. It was observed that using central composite design and moving least square method approach gave the best approximation of the performance levels.

3.4 Application of RSM in seismic performance reliability of reinforced concrete (RC) structures

Shahraki & Shabakhty, (2015) performed numerical case study on the seismic performance reliability of RC frame structures. An integrated algorithm was used which is a combination of improved RSM and a systematic approach for structural system analysis. Factors affecting seismic performance were: Ground motion intensity, gravity loads, material properties. For RSM, Limit state function LSF was defined based on the maximum plastic rotation at the structural component level and first order reliability method FORM was used for calculating performance reliability index and relative importance of random variables. The results showed that a decrease in non-performance probabilities of the structure when the non-performance scenarios were formed at high levels. Also, the integrated algorithm provided seismic performance reliability at different damage levels.

3.5 Use of RSM to generate system level fragilities for existing curved steel bridges

Seo & Linzell, (2013) performed a case study on a group of horizontally curved steel I-girder bridges located in Pennsylvania, New York and Maryland to determine the influence of important parameters on their seismic response and develop system level fragility curves for the bridge group. The developed methodology is then applied to specific bridges. RSM was used to generate the representative bridge systems and utilized fragilities from important bridge seismic components. Results from the study indicated that parameters that significantly influence the seismic fragilities were the number of spans, radius of curvature, and maximum span length. The number of spans and the radius of curvature had the significant influence on fragilities at all damage levels while Span length influenced fragilities at slight to extensive damage levels.

3.6 An application of the RSM in building seismic fragility estimation

An application of the response surface methodology was investigated by Towashiraporn et al. (2008) on a fictitious building of steel moment-resisting frame construction located in downtown Memphis, Tennessee. The input parameter which are most influential on the structure are damping ratio, the yield strength, elastic modulus of the steel and the earthquake intensity while the response variable is the maximum drift ratio. The results indicate that the response surface function correlates with the results obtained from the time-history analyses. The major advantage of the response surface metamodel is to provide a simple functional relation between the most significant input variables and the output (response) and the model is computationally very efficient.

3.7 Probabilistic nonlinear analysis of concrete-faced rock fill (CFR) dams by Monte Carlo simulation (MCS) using RSM

Kartal et al. (2011) used RSM to understand the probabilistic analysis of concrete-faced rock fill (CFR). ANSYS finite element program was used to get displacement and principal stress components. For this study, four different cases were considered; Case 1 concrete slab, rock fill and foundation soil is assumed geometrically and materially linear elastic. Case 2, the first case is considered with geometrically nonlinearity in the whole system. Case 3, materially nonlinear response of rock fill and foundation soil is considered with Case 2. Case 4, materially nonlinear response of the concrete slab is considered with Case 3. Sensitivity analysis was performed to know the most effective parameters on the dam response which were modulus of elasticity, Poisson's ratio and density of 3B and 3C zones and modulus of elasticity of the concrete slab. For the response surface analysis, various experimental design methods were used; star design, full factorial design, central composite design and Box–Behnken design models. Star experimental design with quadratic function was found as the most appropriate model.

3.8 RSM with random factors for seismic fragility of reinforced concrete frames

A study of RSM with random block effects was used to assess the structural capacity of an existing reinforced concrete frame structure. Buratti et al. (2010) used a numerical model to perform a non-linear time-history analyses using a finite element analysis. Different response surface models and simulation plans were implemented, with the aim of achieving a good result between reliability of results and computational saving. The simulation design plans studied were central composite design and 2k factorial designs and the response surface models were quadratic and linear. The results achieved through these models were compared with the results

from full Monte Carlo simulations. It was evident that the quadratic polynomial models are very precise to the design considered and linear models are slightly less accurate in estimating the dependence of the structural capacity.

3.9 Summary

According to Kim et al. (2016) and Mashayekh (2017), beam slope angle has adverse effects on the connection performance of RBS. Such effects are higher strain demand at the heel location and brittle fracture at top flange of the beam. Mohammadi Nia & Moradi, (2020) used statistical analysis to study the effect of beam slope angle and other important factors with their possible interaction. Significant factors were obtained to understand the behaviour of RBS moment connections. This research will use statistical analysis to predict models and optimize these factors including slope angle, beam web slenderness ratio, beam flange slenderness ratio, RBS depth to beam flange width ratio, column flange slenderness ratio in order to improve the structural response of RBS moment connection.

CHAPTER 4

4 PREDICTIVE EQUATIONS FOR RBS MOMENT CONNECTIONS

4.1 General

Five important parameters are identified to have the most significant effects on the response characteristics including slope angle, beam web slenderness ratio, beam flange slenderness ratio, RBS depth to beam flange width ratio, column flange slenderness ratio (Mohammadi Nia & Moradi, 2020). The objective is to derive predictive equations for the response characteristics of RBS connections including Initial stiffness (K_i), Plastic strain index (PI), Moment capacity (M_{max}), Hysteretic energy dissipation (HED), and Strength degradation rate (SDR). A response surface methodology (RSM) is used to generate predictive equations for the response characteristics.

4.2 Response surface methodology (RSM)

Response surface method is a statistical analysis method that analyses the correlation between an experimental response and optimum conditions of input variables which have the greatest effect on the output (Zhao & Tetsuro, 1998). RSM has been effectively applied in many different fields of study such as chemical engineering, industrial engineering, manufacturing, aerospace engineering, structural reliability, and computer simulation (Towashiraporn et al, 2002, 2008). This is used in structural reliability and optimization for a variety of problems. The basic idea is to use the results of a design of experiment to construct a response parameter approximation. This approximation, called the response surface or "metamodel" (model of model), can be built for different parameters of seismic engineering demand. The response surface provides an analytical or explicit function, reliability or optimization performed which can be very fast and requires no additional experiments or simulations (Mohammad et al., 2018).

For efficiency and accuracy, a second-order polynomial is required for the cyclic response of Orthogonal and Non-orthogonal RBS moment connection. The second-order polynomial which can be used is

$$y = \beta_0 + \sum_{i=1}^k \beta_i x_i + \sum_{i=1}^k \beta_{ii} x_i^2 + \sum_{i=1}^{k-1} \sum_{j>1}^k \beta_{ij} x_i x_j + error \quad (\text{Eq. 4.1})$$

where y can be a dependant variable such as seismic response; x_i and x_j are independent variables such as slope angle; β_0 , β_i , β_{ii} , β_{ij} are coefficients to be estimated from the seismic

responses; and k is the experimental design number for the input variables (Huh & Achintya, 2001).

The important component of RSM generally involves three (3) main steps:

- Creating a response surface over a region of interest
- Optimizing the response
- Obtaining a region which yields desirable conditions for multi response variables (Myer et al, 2016).

4.3 Factors and response variables

Five important parameters were chosen for this response surface study. These factors and their ranges are listed in Table 4.1.

Table 4.1. Factors considered in this study

Factor	Symbol	Coded Low (-1)	Coded High (+1)	Unit
Beam web slenderness ratio (λ_{bw})	A	33	52	–
Beam flange slenderness ratio (λ_{bf})	B	5	7	–
Slope angle (θ)	C	0	45	Degree
RBS depth to beam flange width ratio (c/b_{bf})	D	0.1	0.25	–
Column flange slenderness ratio (λ_{cw})	E	16	23.3	–

Note: Adapted from “Effects of design factors on the cyclic response of sloped RBS moment connections” by Moradi, S., & Mohammadi M.N. (2020). *Engineering structures (under review)*.

Five response variables are considered for this response surface study. These response parameters are: Initial stiffness (K_i), Plastic strain index (PI), Moment capacity (M_{max}), Hysteretic energy dissipation (HED), and Strength degradation rate (SDR). Design of experiments is an efficient method of constructing factors combinations. Observation, measurements and computation of a response with factors combinations can be called experiments. Since there are no random errors for computer experiments, some of the methods for the designs with physical experiments might not be ideal for computer-based experiments (Simpson et al. 2001). Therefore, we use an I-optimal design, which is more appropriate for computer experiments (Montgomery 2013). To bridge the disparity between computer experiments and physical experiment an I-optimal design is suitable. I-optimal design is used to choose runs that minimize the integral of the prediction variance across the factor space. A

total of 32 simulation runs of RBS connections with the input parameter combinations were developed and analysed in ANSYS.

4.4 Results and response surface metamodels

Mohammadi Nia & Moradi, (2020) used Design-Expert software package is used to derive the factor combinations. Design-Expert can be used to perform design of experiment such as comparative tests, screening, characterization, optimization, robust parameter design, mixture designs and combined designs. For the purpose of this research, it is used for predicting models and optimizing the structural response of RBS moment connections by locating the best region to achieve goals such as maximizing, minimizing or hitting a target value separately for each response. The factor combinations is shown in Table 4.2 below.

Table 4.2. Factor combinations

Run	A:Beam web slenderness ratio	B:Beam flange slenderness ratio	C:Slope (θ)	D:RBS depth to beam flange width ratio	E:Column flange slenderness ratio
1	47.250	5.78	45.000	0.16750	16.0000
2	52.000	5.00	28.575	0.10000	16.1825
3	39.365	6.79	45.000	0.10000	23.3000
4	33.000	6.31	45.000	0.17350	16.0000
5	52.000	7.00	0	0.12625	20.0150
6	33.000	7.00	18.225	0.10000	17.2775
7	42.500	6.00	22.500	0.17500	19.6500
8	42.215	5.80	23.850	0.17200	19.7595
9	52.000	7.00	45.000	0.10000	16.0000
10	51.050	5.00	45.000	0.17800	23.3000
11	33.000	6.05	19.125	0.10000	22.0590
12	39.175	5.00	0	0.10000	23.3000
13	48.200	6.10	45.000	0.10000	20.0150
14	33.095	5.85	45.000	0.17575	22.9350
15	52.000	6.10	45.000	0.25000	18.9200
16	41.170	5.00	45.000	0.25000	16.0000
17	52.000	7.00	24.750	0.25000	23.3000
18	33.000	5.00	45.000	0.10000	19.9420
19	52.000	6.05	20.250	0.10000	23.3000
20	43.735	6.14	0	0.25000	23.3000
21	42.975	6.05	0	0.10000	16.0000
22	42.215	5.80	23.850	0.17200	19.7595
23	33.000	7.00	45.000	0.25000	21.6210
24	43.165	7.00	28.350	0.17575	19.6358
25	33.000	5.00	27.000	0.25000	23.3000
26	52.000	5.00	0	0.25000	20.0449
27	52.000	6.15	11.925	0.21250	16.0000
28	40.600	7.00	5.625	0.25000	16.0000

Table 4.3. (continued)

Run	A:Beam web slenderness ratio	B:Beam flange slenderness ratio	C:Slope (θ)	D:RBS depth to beam flange width ratio	E:Column flange slenderness ratio
29	33.000	5.00	0	0.18025	16.0000
30	33.000	7.00	0	0.15775	23.3000
31	42.215	7.00	43.875	0.25000	16.0000
32	33.000	6.03	0	0.25000	19.2120

Note: Adapted from “Effects of design factors on the cyclic response of sloped RBS moment connections” by Moradi, S., & Mohammadi M.N. (2020). *Engineering structures (under review)*.

Mohammadi Nia & Moradi, (2020) used mechanical APDL ANSYS software to develop and analyse nonlinear finite element models of RBS connections under cyclic loading. To validate the accuracy of the developed models, two sets of experimental tests (orthogonal and sloped RBS connections) were selected. For verification of the finite element modelling and analysis, the load-rotation and moment-rotation hysteretic curves were compared to the experimental results for the sloped and orthogonal RBS connection respectively. The response values are shown in Table 4.3 below.

Table 4.3. Response values

Run	K_i (N/m)	PI	M_{max} (Nm)	HED (N.m.rad)	SDR
1	1.17787E+09	105.952	8.11979E+06	2.33062E+06	0.858071
2	6.365E+08	110.869	4.92133E+06	1.41509E+06	0.892928
3	1.16674E+09	147.044	7.60821E+06	2.38872E+06	0.841638
4	7.36939E+08	110.066	5.52956E+06	1.68615E+06	1.006570
5	2.8321E+08	71.3179	3.15639E+06	718203	0.860060
6	2.48978E+08	47.0534	2.7165E+06	676844	1.021490
7	4.21951E+08	57.9551	3.53508E+06	1.00156E+06	0.930490
8	4.37381E+08	54.7289	3.59773E+06	675451	0.918685
9	1.38113E+09	150.716	1.00028E+07	2.83942E+06	0.829509
10	1.52261E+09	159.806	8.53309E+06	2.7358E+06	0.860021
11	2.61057E+08	58.4279	2.56087E+06	633577	1.019790
12	1.55034E+08	31.6294	1.85396E+06	447704	1.045480
13	1.36806E+09	138.419	8.82249E+06	1.54946E+06	0.857503
14	8.19097E+08	109.627	5.57339E+06	1.76656E+06	0.990498
15	1.43151E+09	101.588	9.48957E+06	1.42415E+06	0.884505
16	9.05721E+08	91.2457	6.23583E+06	1.65114E+06	0.882387
17	7.11152E+08	86.9772	5.11265E+06	1.52354E+06	0.936306
18	7.15565E+08	124.318	4.95352E+06	1.35205E+06	0.924219
19	5.89882E+08	107.481	4.48906E+06	1.30231E+06	0.860269
20	1.98697E+08	97.6826	1.92681E+06	496049	0.949935
21	1.71644E+08	48.0666	2.2944E+06	507535	1.045620
22	4.37381E+08	54.7289	3.59773E+06	1.02297E+06	0.918685

Table 4.3. (continued)

Run	K_i (N/m)	PI	M_{max} (Nm)	HED (N.m.rad)	SDR
23	1.14239E+09	77.5952	6.06899E+06	1.85943E+06	0.985323
24	6.04135E+08	61.9207	4.87915E+06	1.38961E+06	0.924513
25	3.27194E+08	44.9851	2.59671E+06	762465	1.023180
26	2.31381E+08	134.655	2.28736E+06	562129	1.016200
27	3.18018E+08	90.6536	3.40745E+06	787432	0.896807
28	1.7453E+08	81.0855	2.1619E+06	385776	1.036160
29	9.4111E+07	21.7042	1.29307E+06	276639	1.055690
30	1.33618E+08	26.3848	1.75625E+06	391855	1.051300
31	1.22935E+09	79.6972	7.52974E+06	2.09548E+06	0.881578
32	1.08346E+08	30.4705	1.35153E+06	306422	1.063980

Note: Adapted from “Effects of design factors on the cyclic response of sloped RBS moment connections” by Moradi, S., & Mohammadi M.N. (2020). *Engineering structures (under review)*.

4.4.1 Initial stiffness (K_i)

The initial stiffness (K_i) represents the secant stiffness of the RBS connection at the drift ratio of 0.4% and connections models ranges from 9.41E+07 N/m to 1.52E+09 N/m. The response surface model for K_i was fitted with a two-factor interaction model shown in Eq. 4.2:

$$\begin{aligned}
 K_i = & -1659332938 + (26922428 * A) + (63593934 * B) + (-52631237 * C) \\
 & + (101837805 * E) + (596591 * AC) + (1979583 * BC) \\
 & + (577094 * CE) + (495293 * C^2) \qquad \qquad \qquad (Eq. 4.2)
 \end{aligned}$$

This metamodel can be used to predict the initial stiffness of connections models and insignificant terms with a p -value greater than 0.05 were removed from the predictive equation when fitting the model. ANOVA shows R^2 and adjusted- R^2 values of 0.99 and 0.98, respectively. High values of R^2 and adjusted- R^2 indicate that the metamodel is a good approximation for the response over the design space.

Figure 4.1 shows 3D plots of K_i response with respect to input parameters. The plots show that the initial stiffness (K_i) of the moment connection is increased by increasing the slope angle while other factors remain at their mean values. Therefore, a higher beam slope angle leads to stiffer connections. Refer to appendix for more information on the 3D plots of initial stiffness response with respect to input parameters.

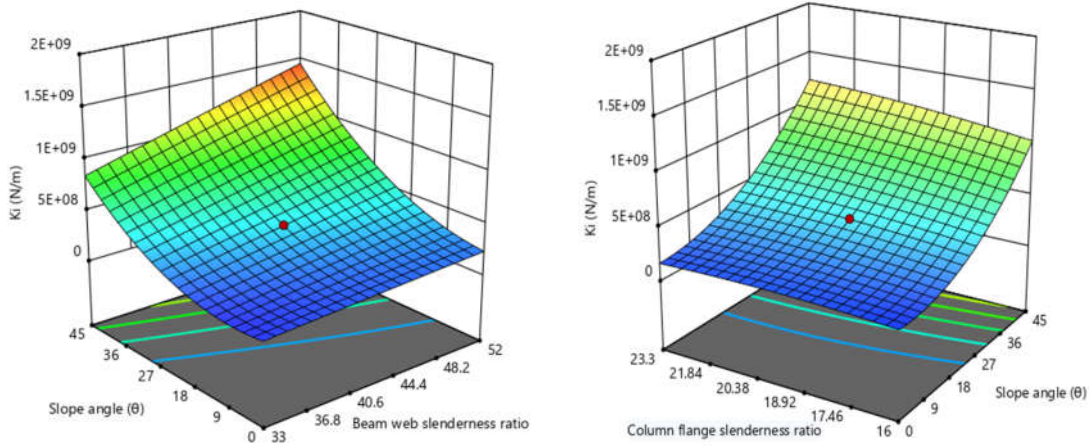


Figure 4.1. Variation of initial stiffness response variable to different factors

4.4.2 Equivalent Plastic Strain Index (PI)

Plastic Strain index (*PI*), indicates the local inelastic strain demand and it is obtained for connection models at 4% drift ratio. The connection model *PI* ranges from 21.7 to 159.86, in the metamodel (Eq. 4.3). Insignificant terms with *p-values* greater than 0.05 was removed.

$$PI = 32.4458 + (2.01 * A) + (4.20 * C) + (-0.97 * AB) + (-0.06 * AC) + (-13.9 * CD) + (0.04 * C^2) + (0.99 * E^2) \quad (Eq. 4.3)$$

The R^2 and adjusted- R^2 values of model is 0.98 and 0.96, respectively. This metamodel can be used to predict the plastic strain index of the moment connection. Figure 4.2 shows 3D plots of *PI* response with respect to input parameters. The plots show that the increase in plasticity index (*PI*) of the moment connection occurs with higher slope angle and beam web slenderness ratio which indicates higher inelastic strain demands. Refer to appendix for more information on the 3D plots of plastic strain index with respect to input parameters.

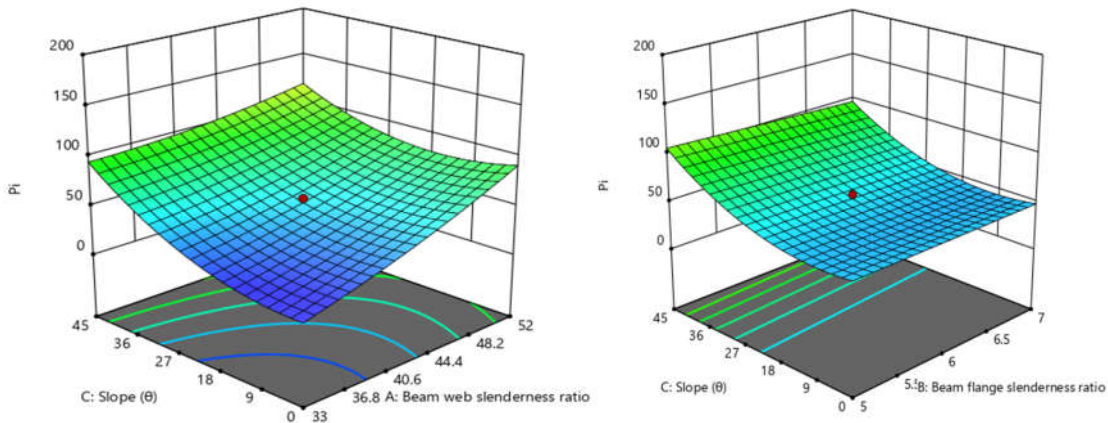


Figure 4.2. Variation of plastic strain index with respect to different factors

4.4.3 Moment capacity (M_{max})

Moment capacity (M_{max}) is the peak moment resistance of the RBS connection. The moment capacity (M_{max}) of the RBS connection ranges from $1.29E+06$ Nm to $1.0E+07$ Nm. A quadratic model was used to fit the response surface model. The R^2 and adjusted- R^2 values of model is 0.99 and 0.99, respectively. This metamodel can be used to predict the moment capacity of moment connection.

$$\begin{aligned}
 M_{max} = & -9.98E + 06 + (34212.6 * A) + (1.38E + 06 * B) + (-218838 * C) \\
 & + (5.03E + 06 * D) + (550708 * E) + (-2002.13 * AE) \\
 & + (9387.65 * BC) + (-1.81E + 06 * BD) + (-27922.9 * BE) \\
 & + (53309.5 * CD) + (1142.48 * CE) + (2438.38 * C^2) \\
 & + (-7247.1 * E^2)
 \end{aligned}
 \tag{Eq. 4.4}$$

Figure 4.3 illustrates the effects of factor's interaction on the moment capacity. From the 3D plots, it is observed that the slope angle has a relatively higher influence on the moment capacity of the connection compared with the other significant factors. Therefore, increasing slope angle can increase moment capacity of the connection. Refer to appendix for more information on the 3D plots of moment capacity with respect to input parameters.

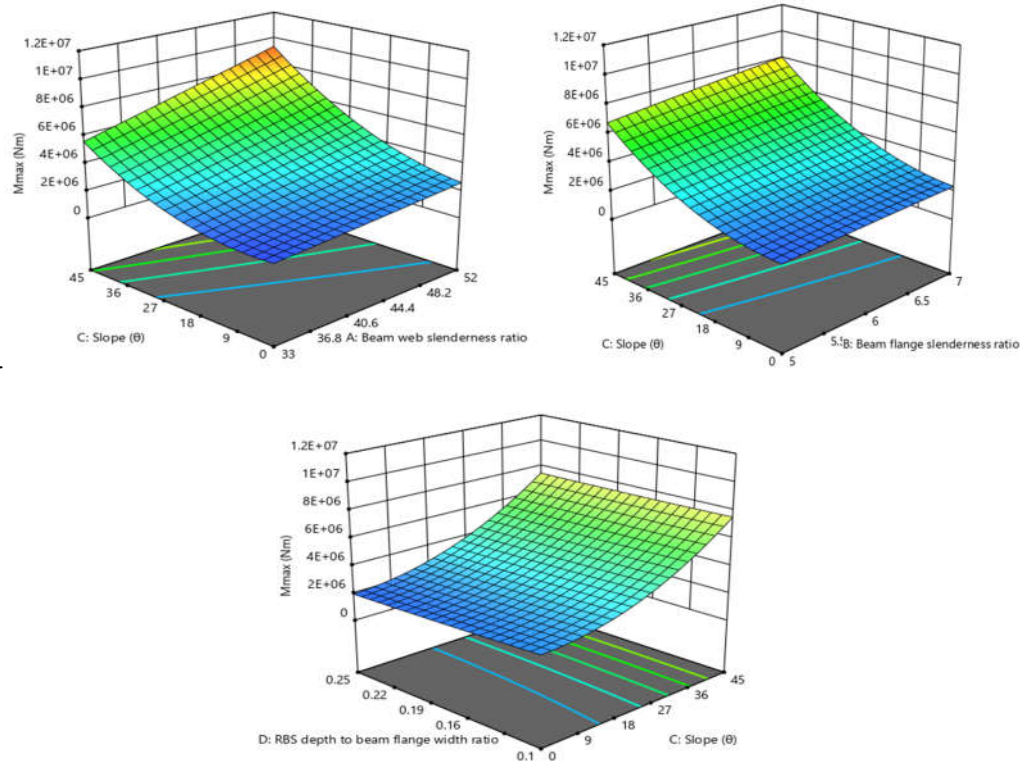


Figure 4.3. Variation of moment capacity with respect to different factors

4.4.4 Hysteretic energy dissipation (HED)

Hysteretic energy dissipation (*HED*) corresponds to the total area enclosed by the hysteretic curve up to 4% drift ratio. *HED* ranged from 276639N.m.rad to 2.84E+06N.m.rad. For an adequate R^2 and adjusted- R^2 values the model was transformed (inverse) and the R^2 and adjusted- R^2 values of model is 0.99 and 0.96, respectively. This metamodel can be used to predict the Hysteretic energy dissipation.

$$\ln(HED) = 16.29 + (0.10 * A) + (0.05 * C) + (-0.001 * AC) \quad (Eq. 4.5)$$

Figure 4.4 illustrates the effects of the factor's interaction on hysteretic energy dissipation. From the 3D plots, it observes that by increasing the slope angle, the dissipated energy also increased. Refer to appendix for more information on the 3D plots of hysteretic energy dissipation with respect to input parameters.

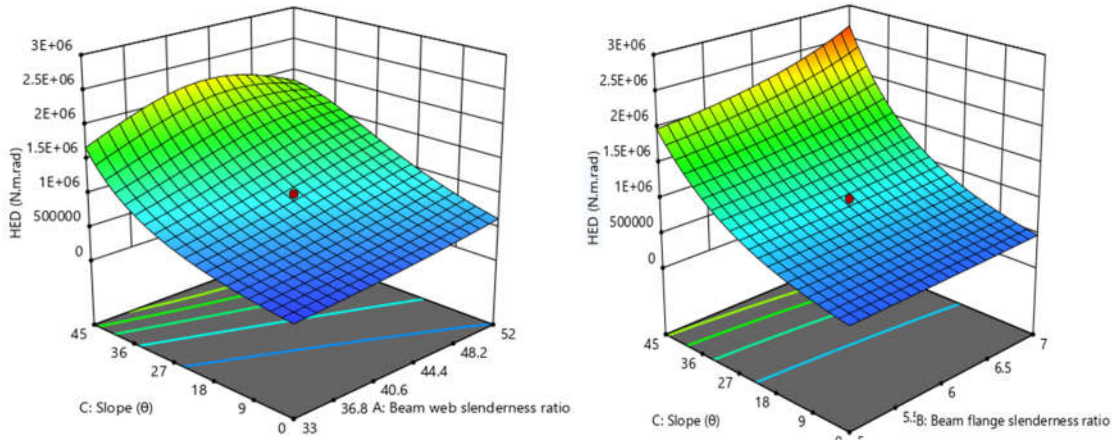


Figure 4.4. Variation of hysteretic energy dissipation with respect to different factors

4.4.5 Strength degradation rate (SDR)

Strength degradation rate (*SDR*) is due to the occurrence of buckling in the connection specimen. An *SDR* less than one indicates the occurrence of strength degradation, *SDR* ranges from 0.83 to 1.06. The R^2 and adjusted- R^2 values of the model is 0.83 and 0.75, respectively. This metamodel can be used to predict the Strength degradation.

$$SDR = 1.50 + (-0.02 * A) + (-0.01 * C) \quad (Eq. 4.6)$$

Figure 4.5 illustrates the effects of the factor's on Strength degradation rate. From the 3D plots, it observes that by increasing the slope angle and decreasing beam web slenderness ratio, low strength degradation rate can be achieved.

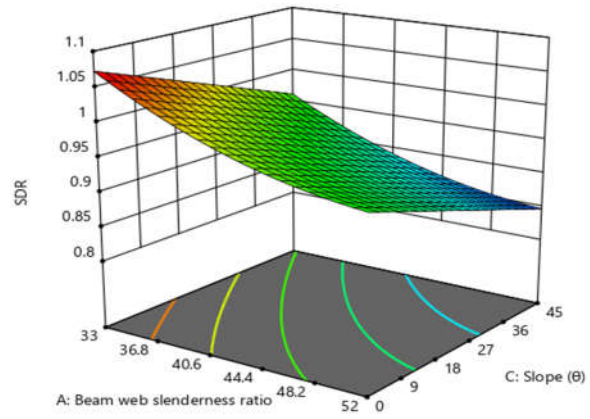


Figure 4.5. Variation of strength degradation with respect to beam slope angle and beam web slenderness ratio

CHAPTER 5

5 MULTIPLE RESPONSE OPTIMIZATION

5.1 General

Analysing the relationship between response and important factors, the metamodels generated can be used for response optimization. Optimization is useful for finding the range of factors where optimum conditions can be achieved. For a multiple response optimization, desirability functions are used. Six optimizations analyse are discussed in this chapter and the goals for the optimization is to find a threshold of the beam slope angle in which fracture and high inelastic demand will occur with respect to maximizing the connection. The following sections include a background information of multiple-response optimization and desirability functions. Design-Expert software is used to determine the best factor settings, in which the most desirable or optimum conditions can be achieved.

5.2 Desirability function for multiple response optimization.

Derringer and Suich (1980) introduced approach for selecting between alternatives which is used for simultaneous optimization technique. For a desirability function, d_i , is defined for each response variable. The desirability function varies from 0 to 1:

$$0 \leq d_i \leq 1$$

where if the objective is at its goal or target, then $d_i = 1$, and if the response is outside an acceptable region, $d_i = 0$. Desirability functions involving maximizing an overall desirability function, D (Myers et al. 2016):

$$D = (d_1 \times d_2 \times \dots \times d_n)^{1/n} \quad (\text{Eq. 5.1})$$

where n is the number of responses.

For maximizing a response, the desirability function is

$$d = \begin{cases} 0 & y < l \\ \left(\frac{y-L}{T-L}\right)^r & L \leq y \leq T \\ 1 & y > T \end{cases} \quad (\text{Eq. 5.2})$$

where T and L are the target and lower bounds respectively. If the weight $r = 1$, the desirability function is linear.

For minimizing a response, the desirability function is

$$d = \begin{cases} 1 & y < T \\ \left(\frac{U-y}{U-T}\right)^r & T \leq y \leq U \\ 1 & y > U \end{cases} \quad (\text{Eq. 5.3})$$

For making a response close to its possible target value, the desirability function is

$$d = \begin{cases} 0 & y < L \\ \left(\frac{y-L}{T-L}\right)^{r_1} & L \leq y \leq T \\ \left(\frac{U-y}{U-T}\right)^{r_2} & T \leq y \leq U \\ 1 & y > U \end{cases} \quad (\text{Eq. 5.4})$$

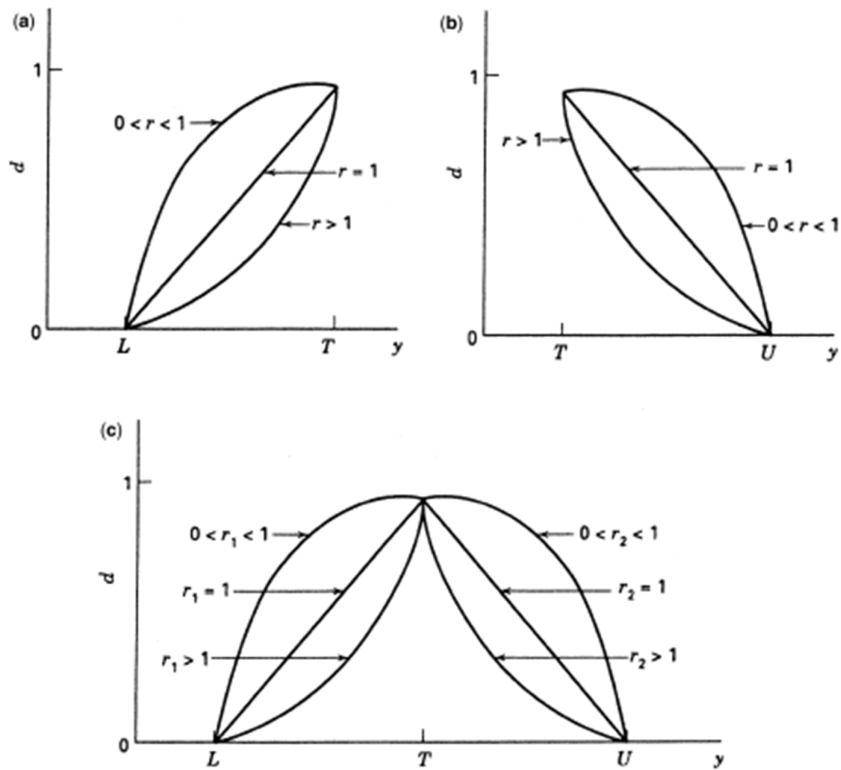


Figure 5.1. The desirability function when the optimization goal is to: (a) maximize the response; (b) minimize the response; (c) assign a target for the response (Myers et al. 2016).

5.3 Optimization objectives

For the optimization of RBS moment connection, six different objectives were considered. Design-Expert software uses a weight of 1 for the optimization objectives. Also to make emphasis on a response, using a weight of 10 would cause the optimization to aim for a solution that is close to or beyond the stated objective.

First optimization aimed at improving the structural response characteristics by maximizing initial stiffness (K_i), moment capacity (M_{max}), hysteretic energy dissipation (HED), and strength degradation rate (SDR) and minimizing plastic strain index (PI). All weights were equal to 1 except for plastic strain index (PI). A weight of 10 was used to emphasize the minimization of plastic strain index (PI) which is important for reducing the inelastic strain demand in RBS connection.

Second optimization is to improve structural response characteristics by maximizing moment capacity (M_{max}), hysteretic energy dissipation (HED), and strength degradation rate (SDR). All weight were equal to 1 except for strength degradation rate. A weight of 10 was used to emphasize the maximization of strength degradation rate. It is important for strength degradation rate to be greater than 1 for RBS connections to minimise the occurrence of buckling and strength degradation under earthquake loading.

Third optimization aimed at improving the structural response characteristics by maximising hysteretic energy dissipation (HED), strength degradation rate (SDR) and minimising plastic strain index (PI). A weight of 10 was used to emphasis the minimization of plastic strain index (PI) which is important for reducing the inelastic strain demand in RBS connection while ensuring low strength degradation rate and increased energy dissipation.

Fourth optimization goal is knowing the range of beam slope angle at which plastic strain index (PI) can be minimized. Fifth optimization aimed at finding the range of beam slope angle which low strength degradation rate can occur. Sixth optimization goal is aimed at minimizing plastic strain index (PI) and maximizing strength degradation rate (SDR).

Table 5.1. Objectives and constraints for the first optimization analysis

Factor and Response	Goal	Lower Limit	Upper Limit	Unit	Weight
Beam web slenderness ratio	is in range	33	52	-	1
Beam flange slenderness ratio	is in range	5	7	-	1
Slope (θ)	is in range	0	45	degree	1
RBS depth to beam flange width ratio	is in range	0.1	0.25	-	1
Column flange slenderness ratio	is in range	16	23.3	-	1
K_i	maximize	9.41E+07	1.52E+09	N/m	1

Table 5.1. (continued)

PI	minimize	21.704	159.806	-	10
Mmax	maximize	1.29E+06	1.00E+07	N.m	1
HED	maximize	276639	2.84E+06	N.m.rad	1
SDR	maximize	0.830	1.064	-	1

Table 5.2. Objectives and constraints for the second optimization analysis

Factor and Response	Goal	Lower Limit	Upper Limit	Unit	Weight
Beam web slenderness ratio	is in range	33	52	-	1
Beam flange slenderness ratio	is in range	5	7	-	1
Slope (θ)	is in range	0	45	degree	1
RBS depth to beam flange width ratio	is in range	0.1	0.25	-	1
Column flange slenderness ratio	is in range	16	23.3	-	1
Mmax	maximize	1.29E+06	1.00E+07	N.m	1
HED	maximize	276639	2.84E+06	N.m.rad	1
SDR	maximize	0.830	1.064	-	10

Table 5.3. Objectives and constraints for the third optimization analysis

Factor and Response	Goal	Lower Limit	Upper Limit	Unit	Weight
Beam web slenderness ratio	is in range	33	52	-	1
Beam flange slenderness ratio	is in range	5	7	-	1
Slope (θ)	is in range	0	45	degree	1
RBS depth to beam flange width ratio	is in range	0.1	0.25	-	1
Column flange slenderness ratio	is in range	16	23.3	-	1
PI	minimise	21.704	159.806	-	10
HED	maximize	276639	2.84E+06	N.m.rad	1
SDR	maximize	0.830	1.064	-	1

Table 5.4. Objectives and constraints for the fourth optimization analysis

Factor and Response	Goal	Lower Limit	Upper Limit	Unit	Weight
Beam web slenderness ratio	is in range	33	52	-	1
Beam flange slenderness ratio	is in range	5	7	-	1
Slope (θ)	is in range	0	45	degree	1
RBS depth to beam flange width ratio	is in range	0.1	0.25	-	1
Column flange slenderness ratio	is in range	16	23.3	-	1
PI	minimize	21.704	159.806	-	1

Table 5.5. Objectives and constraints for the fifth optimization analysis

Factor and Response	Goal	Lower Limit	Upper Limit	Unit	Weight
Beam web slenderness ratio	is in range	33	52	-	1
Beam flange slenderness ratio	is in range	5	7	-	1
Slope (θ)	is in range	0	45	degree	1
RBS depth to beam flange width ratio	is in range	0.1	0.25	-	1
Column flange slenderness ratio	is in range	16	23.3	-	1
SDR	maximise	0.830	1.064	-	1

Table 5.6. Objectives and constraints for the sixth optimization analysis

Factor and Response	Goal	Lower Limit	Upper Limit	Unit	Weight
Beam web slenderness ratio	is in range	33	52	-	1
Beam flange slenderness ratio	is in range	5	7	-	1
Slope (θ)	is in range	0	45	degree	1
RBS depth to beam flange width ratio	is in range	0.1	0.25	-	1
Column flange slenderness ratio	is in range	16	23.3	-	1
PI	minimize	21.704	159.806	-	1
SDR	maximise	0.830	1.064	-	1

5.4 Results and discussions

5.4.1 Results of the first optimization analysis

The optimum regions of the design space for the structural response characteristics can be determined from the results of the optimization. The optimal parameter achieved are beam web slenderness ratio = 33, beam flange slenderness ratio = 7, slope angle = 27.82°, RBS depth to beam flange width ratio = 0.25, column flange slenderness ratio = 20.44. The overall desirability function for this parameter combination is 0.332. The desirability selection for each of the response is based on Equation 5.2 and Equation 5.3 while the overall parameter is based on Equation 5.1. The goal is not necessary for desirability to be 1 but to determine the optimum sets of input parameters. For the desirability of each responses is in the table 5.7.

Table 5.7 Responses with their desirability

Response	Desirability
Initial stiffness (K_i),	0.29
Plastic strain index (PI),	0.22
Moment capacity (M_{max}),	0.21
Hysteretic energy dissipation (HED)	0.50
Strength degradation rate (SDR)	0.80

Figure 5.2 presents one-factor desirability plots at the optimal condition when desirability is 0.332. These plots illustrate the variation of desirability function changes with respect to each factor. For an optimal range for each factor where most desirable response are achieved; 80% of the maximum desirability will be used ($80\% \times 0.332 = 0.27$).

From Figure 5.2(a) shown below, the desirability function is decreased from 0.33 to 0.11 by 30 increasing the beam web slenderness ratio from low level to high level. The optimal range for beam web slenderness ratio is from 33 to 41.

Larger beam flange slenderness ratio is found to more desirable as shown in Figure 5.2(b). The desirability function remains higher than 0.27 over its entire range. Beam flange slenderness ratio is not very important for reaching the optimization goals.

Figure 5.2(c) suggests that beams slope at 27.8° is beneficial at optimizing the RBS moment connections by minimising PI. For a desirability ($D \geq 0.27$) beam slope angle ranged between 16 and 38.

From Figure 5.2(d), higher RBS depth to beam flange width ratio are more desirable when the reaching the goal of the optimised response characteristics. A desirability value above 27% is when RBS depth to beam flange width ratio is between 0.177 and 0.25.

Figure 5.2(e) indicates that column flange slenderness ratio achieved a higher desirability value at 20.44. Furthermore, it was observed that increasing column flange slenderness ratio the desirability decreased till 23.3. The optimal ranges of column flange slenderness ratio are 17.16 to 23.3.

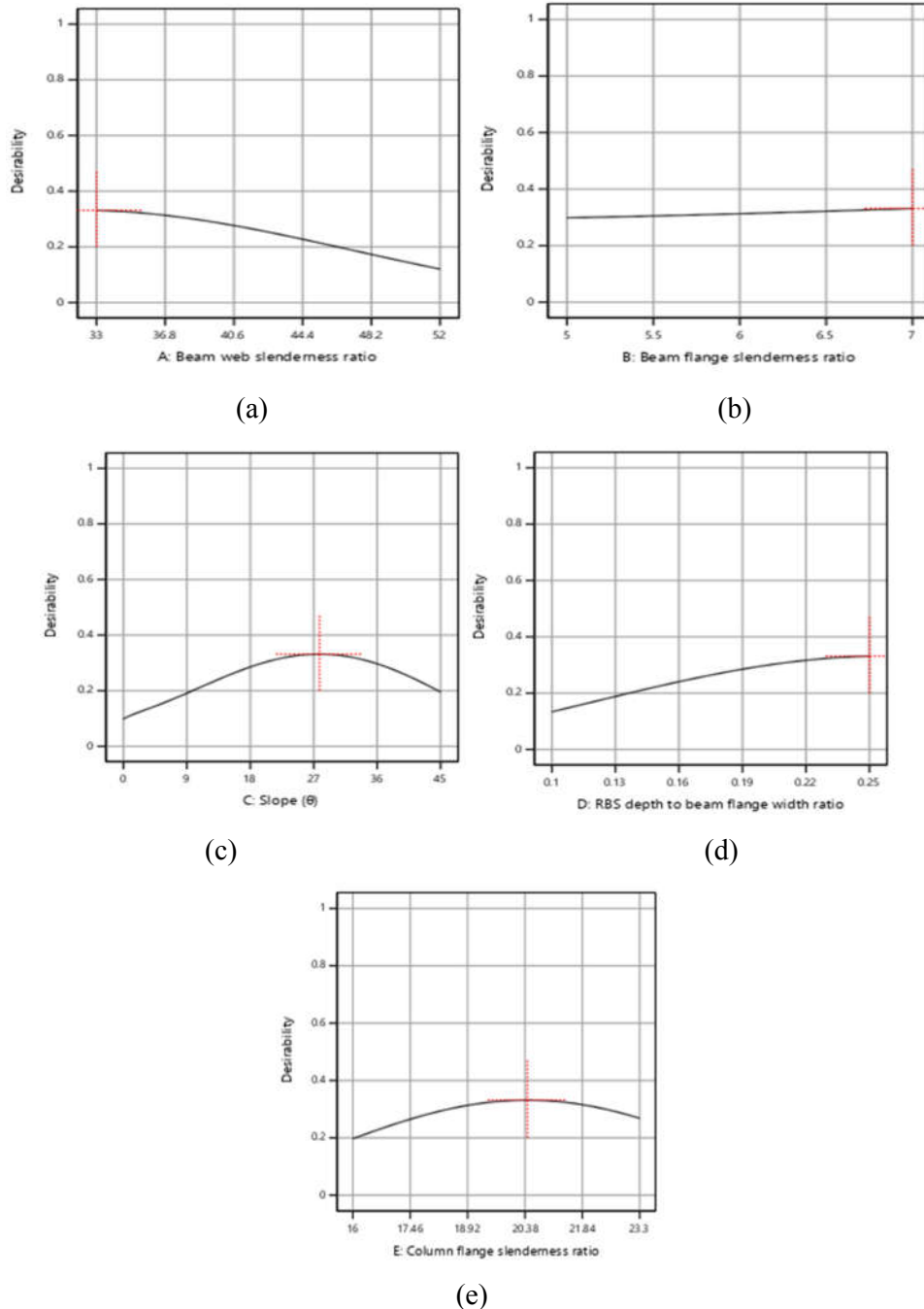


Figure 5.2. First optimization analysis, the desirability function at the optimum condition versus: (a) beam web slenderness ratio; (b) beam flange slenderness ratio, (c) slope angle; (d) RBS depth to beam flange width ratio; (e) column flange slenderness ratio

Figure 5.3 shows the contours plots of the desirability functions for different factors. The optimal conditions with desirability of 27%. The contours plot further support the optimization results illustrated above.

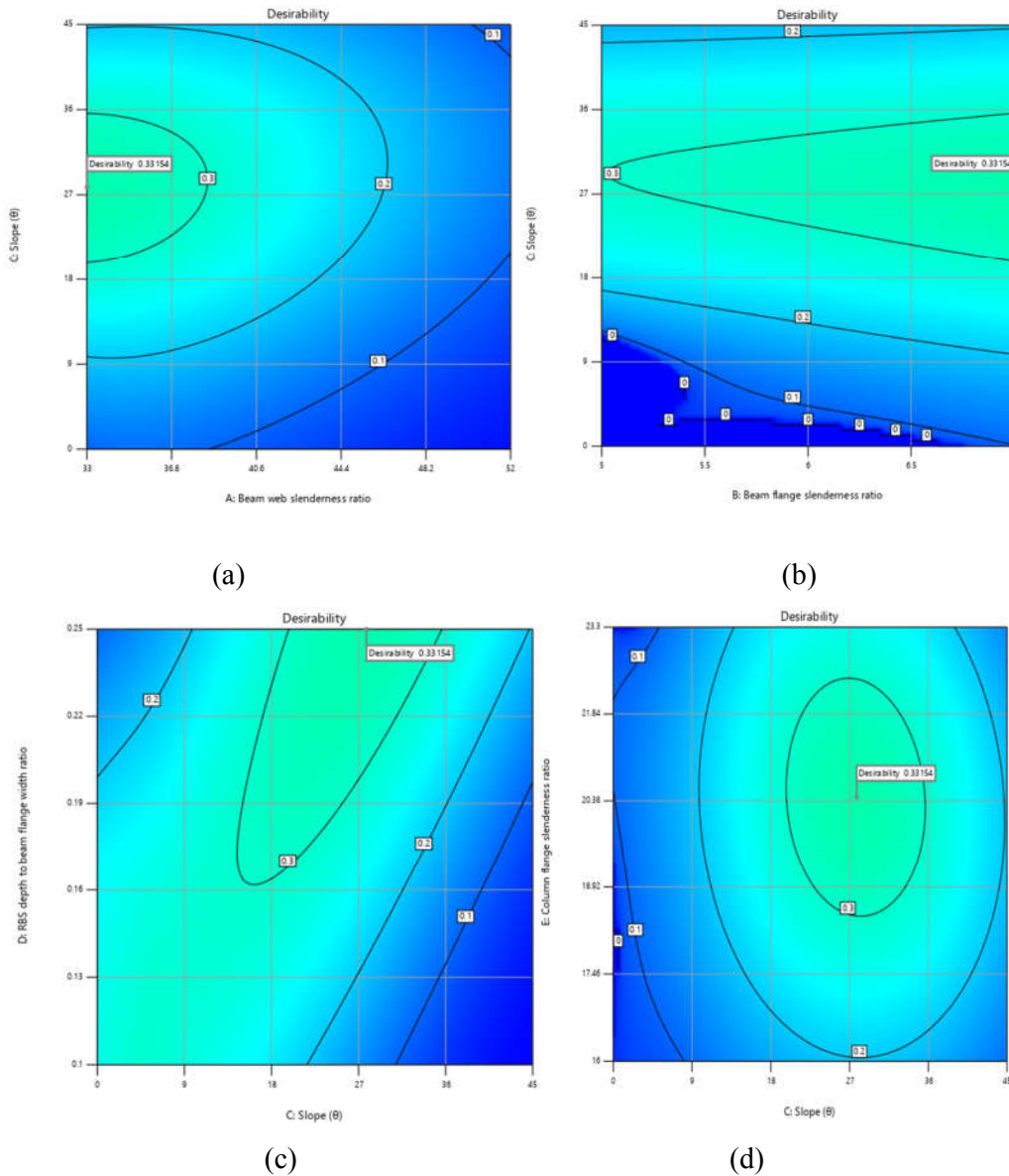


Figure 5.3. Contour plot of desirability at the optimum condition: (a) beam slope versus beam web slenderness ratio; (b) beam slope versus beam flange slenderness ratio; (c) beam slope versus RBS depth to beam flange width ratio; (d) beam slope versus column flange slenderness ratio.

5.4.2 Results of the second optimization analysis

The optimum regions of the design space determined the best structural response characteristics where higher strength degradation rate can be achieved. The optimal parameter achieved are

beam web slenderness ratio = 33, beam flange slenderness ratio = 7, slope angle = 21.52°, RBS depth to beam flange width ratio = 0.11, column flange slenderness ratio = 23.3. The overall desirability function for this parameter combination is 0.26. For the desirability of each responses is in the Table 5.8.

Table 5.8 Responses with their desirability

Response	Desirability
Moment capacity (M_{max}),	0.19
Hysteretic energy dissipation (HED)	0.50
Strength degradation rate (SDR)	0.18

Figure 5.4 presents one-factor desirability plots at the optimal condition when desirability is 0.26. These plots illustrate the variation of desirability function changes with respect to each factor. For an optimal range for each factor where most desirable response are achieved; 80% of the maximum desirability will be used ($80\% \times 0.26 = 0.21$).

Figure 5.4(a), the desirability function is decreased from 0.26 to 0 by increasing the beam web slenderness ratio from low level to high level. The optimal range for beam web slenderness ratio is from 33 to 34.

Larger beam flange slenderness ratio is found to more desirable as shown in Figure 5.4(b). For a desirability ($D \geq 0.21$) beam flange slenderness ratio ranged from (6.3 to 7).

Figure 5.4(c) suggests that the desirability function is not much affected by the beam slope angle but beams slope at 21.52° is beneficial at have a low strength degradation rate and increasing optimization of RBS moment connections. A desirability value ($D \geq 0.21$) beam slope angle ranged between 0° and 44°.

Figure 5.4(d), lower RBS depth to beam flange width ratio are more desirable when the reaching the goal of the optimised response characteristics. A desirability value above 21% is achieved through the entire range of RBS depth to beam flange width ratio.

Figure 5.4(e) suggests that the desirability value above 21% is achieved through the entire range of column flange slenderness ratio. The desirability function is insensitive to the column flange slenderness ratio.

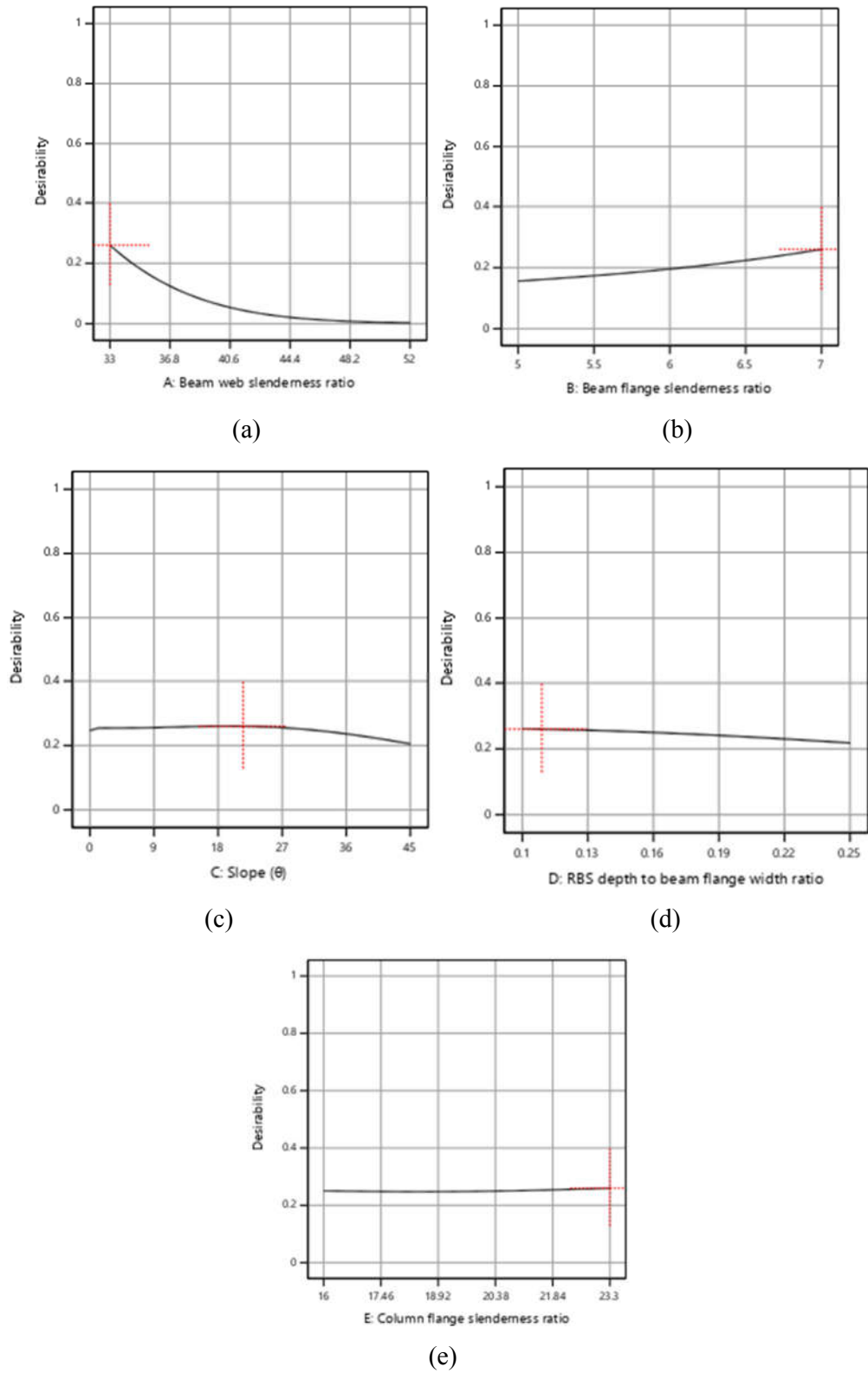


Figure 5.4. Second optimization analysis, the desirability function at the optimum condition versus: (a) beam web slenderness ratio; (b) beam flange slenderness ratio, (c) slope angle; (d) RBS depth to beam flange width ratio; (e) column flange slenderness ratio.

Figure 5.5 shows the contours plots of the desirability functions for different factors. The optimal conditions with desirability of 26%. The contours plot further support the optimization results illustrated above.

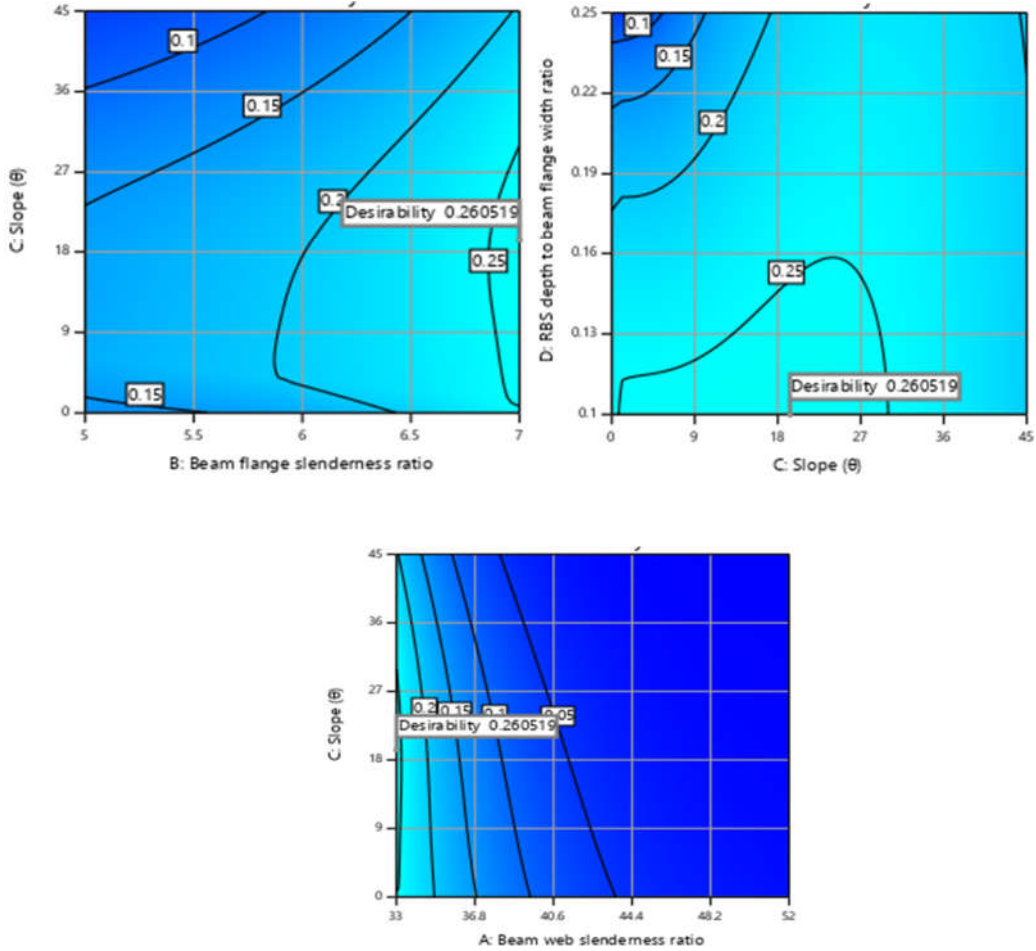


Figure 5.5. Contour plot of desirability at the optimum condition: (a) beam slope versus beam flange slenderness ratio; (b) RBS depth to beam flange width ratio versus beam slope; (c) beam slope versus beam web slenderness ratio.

5.4.3 Results of the third optimization analysis

Third optimization analysis aimed at improving the structural response characteristics by maximizing hysteretic energy dissipation (*HED*), and strength degradation rate (*SDR*) minimising plastic strain index (*PI*). The optimum regions of the design space determined the best structural response characteristics where higher strength degradation rate and low plastic strain index can be achieved. The optimal parameter achieved are beam web slenderness ratio = 33, beam flange slenderness ratio = 5, slope angle = 20°, RBS depth to beam flange width

ratio = 0.176, column flange slenderness ratio = 19.2. The overall desirability function for this parameter combination is 0.634. For the desirability of each responses is in the Table 5.9.

Table 5.9. Responses with their desirability

Response	Desirability
Plastic strain index (<i>PI</i>),	1
Hysteretic energy dissipation (<i>HED</i>)	0.32
Strength degradation rate (<i>SDR</i>)	0.82

Figure 5.6 presents one-factor desirability plots at the optimal condition when desirability is 0.634. These plots illustrate the variation of desirability function changes with respect to each factor. For an optimal range for each factor where most desirable response are achieved; 80% of the maximum desirability will be used ($80\% \times 0.634 = 0.51$).

Figure 5.6(a) shown below, lower beam web slenderness ratio is desirable for the optimum condition for this problem. The desirability function is decreased from 0.634 to 0.05 by increasing the beam web slenderness ratio from low level to high level. The optimal range for beam web slenderness ratio is from 33 to 36.

Lower beam flange slenderness ratio is found to more desirable as shown in Figure 5.6(b). For a desirability ($D \geq 0.51$) beam flange slenderness ratio ranged from (5 to 6.3).

Figure 5.6(c) suggests that desirability function ($D \geq 0.51$) ranges between 8° and 26° . The maximum desirability of slope angle is achieved at 20° however it was observed that desirability reduces when beams slope greater than 20° .

Figure 5.6(d), a desirability value above 51% is achieved from 0.11 to 0.25. RBS depth to beam flange width ratio at 0.17 is most desirable when the reaching the goal of the optimised response characteristics.

Figure 5.6(e) indicates that desirability decreases when column flange slenderness ratio greater than 22.3. Therefore, high column flange slenderness ratio is more desirable when the reaching the goal of the optimised response characteristics.

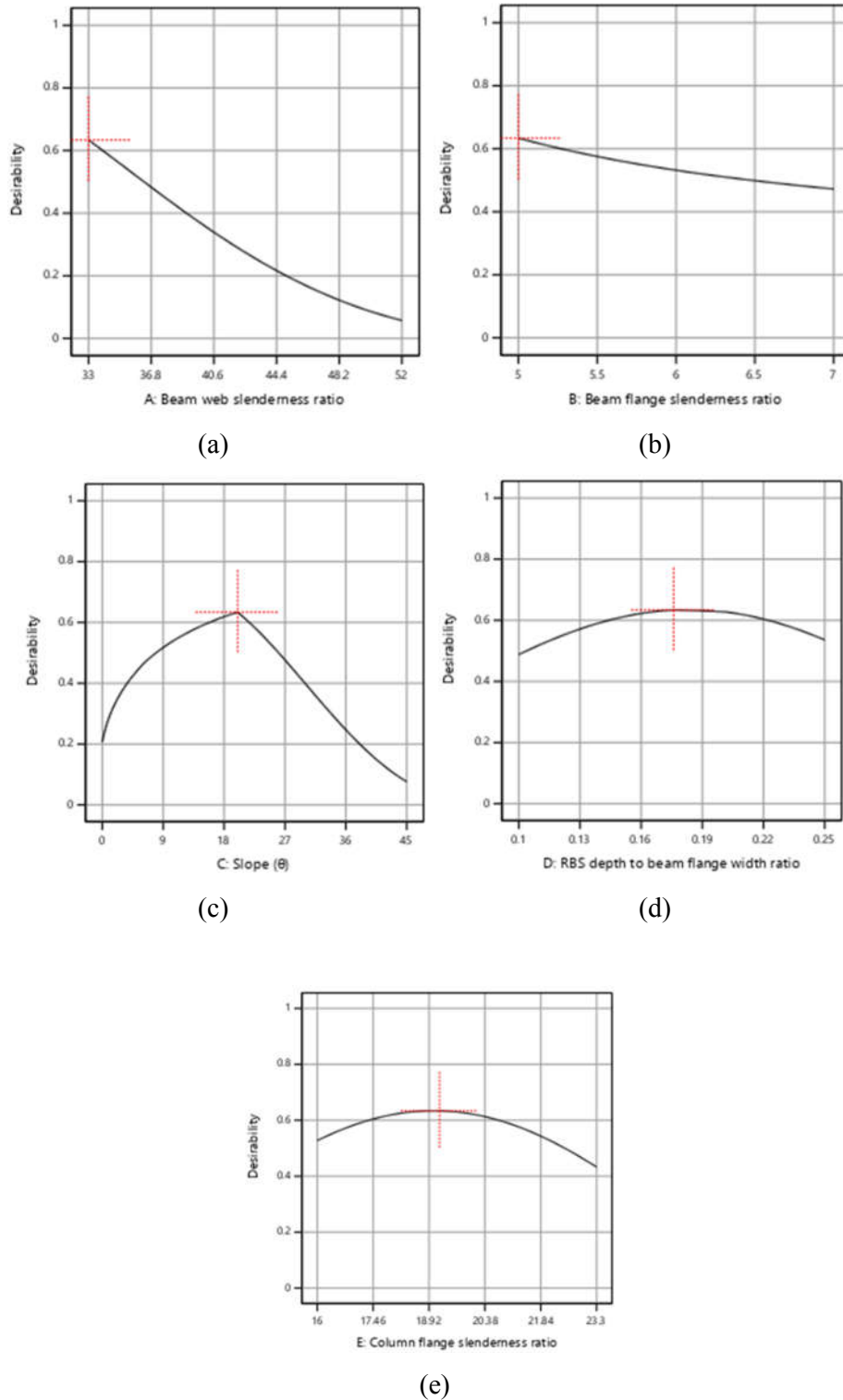


Figure 5.6. Third optimization analysis, the desirability function at the optimum condition versus: (a) beam web slenderness ratio; (b) beam flange slenderness ratio, (c) slope angle; (d) RBS depth to beam flange width ratio; (e) column flange slenderness ratio

Figure 5.7. shows the contours plots of the desirability functions for different factors. The optimal conditions with desirability of 63.4%. The contours plot further support the optimization results illustrated above.

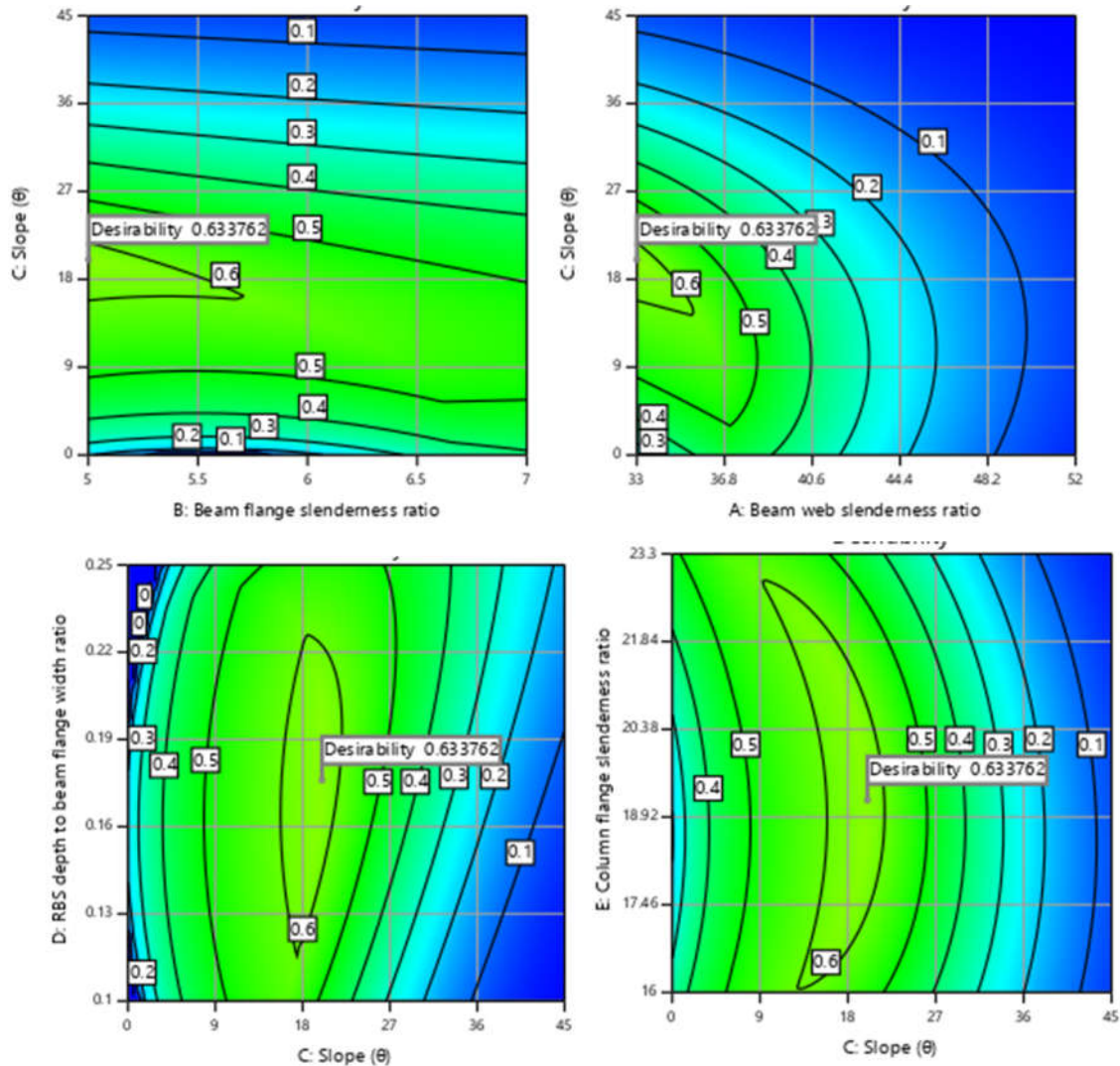


Figure 5.7. Contours plots of the desirability functions for different factors.

5.4.4 Results of the fourth optimization analysis

The fourth optimization analysis aimed at improving the structural response characteristics by only minimising plastic strain index (PI). The optimum regions of the design space determined the best structural response characteristics where low plastic strain index can be achieved. The optimal parameter achieved is are, beam web slenderness ratio = 33.04, beam flange slenderness ratio = 5, slope angle = 11.87°, RBS depth to beam flange width ratio = 0.237, column flange slenderness ratio = 20.2. The overall desirability function for this parameter combination is 1.

Figure 5.8 presents one-factor desirability plots at the optimal condition when desirability is 1. These plots illustrate the variation of desirability function changes with respect to each factor. For an optimal range for each factor where most desirable response are achieved; 80% of the maximum desirability will be used ($80\% \times 1 = 0.80$).

Figure 5.8(a) shows that above, lower beam web slenderness ratio is desirable for the minimising plastic strain index (PI). The desirability function is decreased by increasing the beam web slenderness ratio from low level to high level. The optimal range for beam web slenderness ratio is from 33 to 40.16.

Lower beam flange slenderness ratio is found to more desirable as shown in Figure 5.8(b), however the desirability function remains higher than 0.8 over its entire range.

Figure 5.8(c) suggests that maximum desirability was achieved at 11.87° , however a decrease in the desirability value was observed from 11.87° to 45° . The desirability range for beam slope angle ($D \geq 0.8$) is 0° to 36° .

Figure 5.8(d), the desirability function is not sensitive to RBS depth to beam flange width ratio as desirability value above 80% was achieved through the entire range of RBS depth to beam flange width ratio.

Figure 5.8(e), maximum desirable value was achieved between 18.3 and 20.3. Desirability value above 80% was achieved through the entire range column flange slenderness ratio.

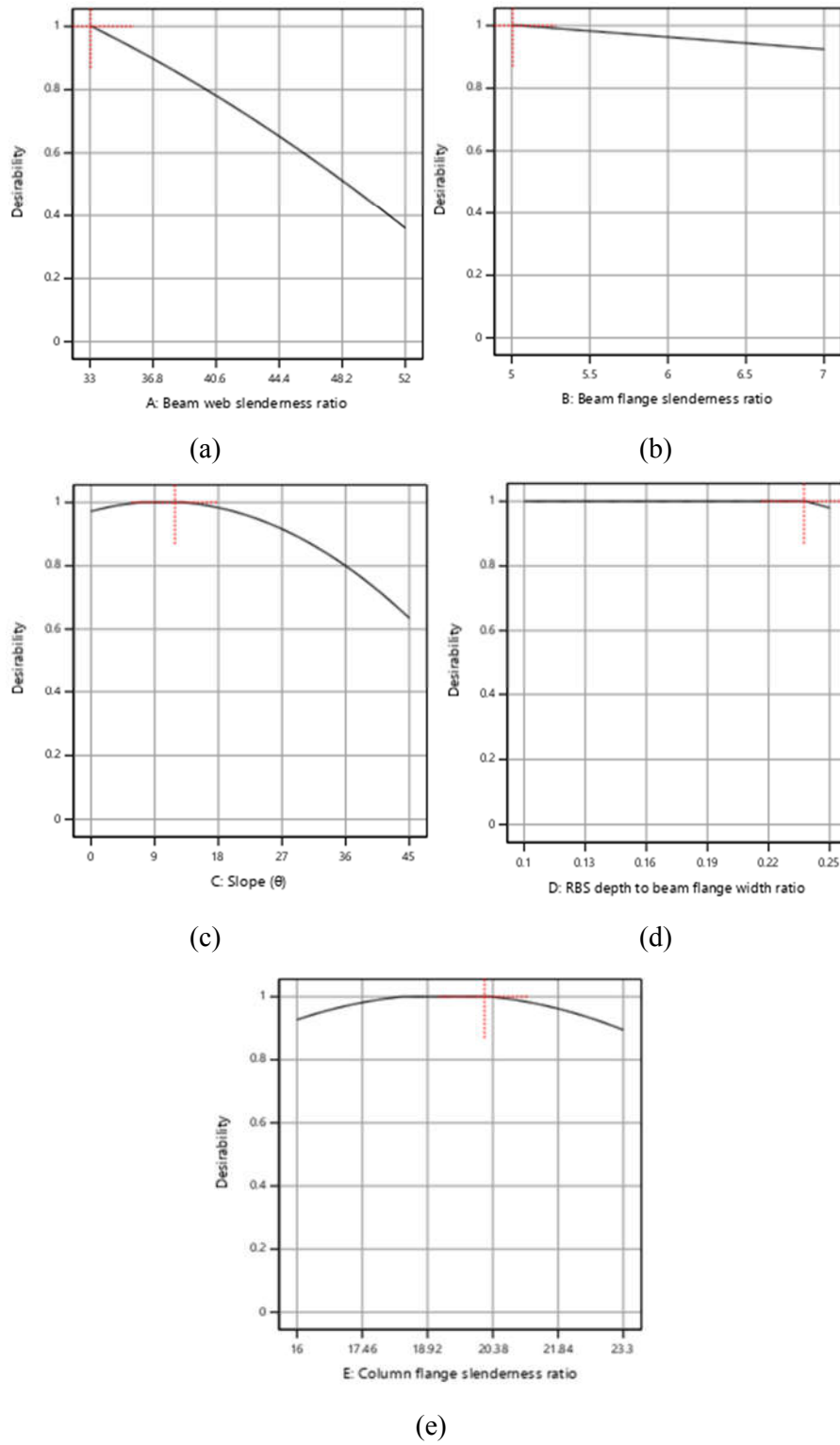


Figure 5.8. Fourth optimization analysis, the desirability function at the optimum condition versus: (a) beam web slenderness ratio; (b) beam flange slenderness ratio, (c) slope angle; (d) RBS depth to beam flange width ratio; (e) column flange slenderness ratio

Figure 5.9. shows the contours plots of the desirability functions for different factors. The optimal conditions with desirability of 100%. The contours plot further support the optimization results illustrated above.

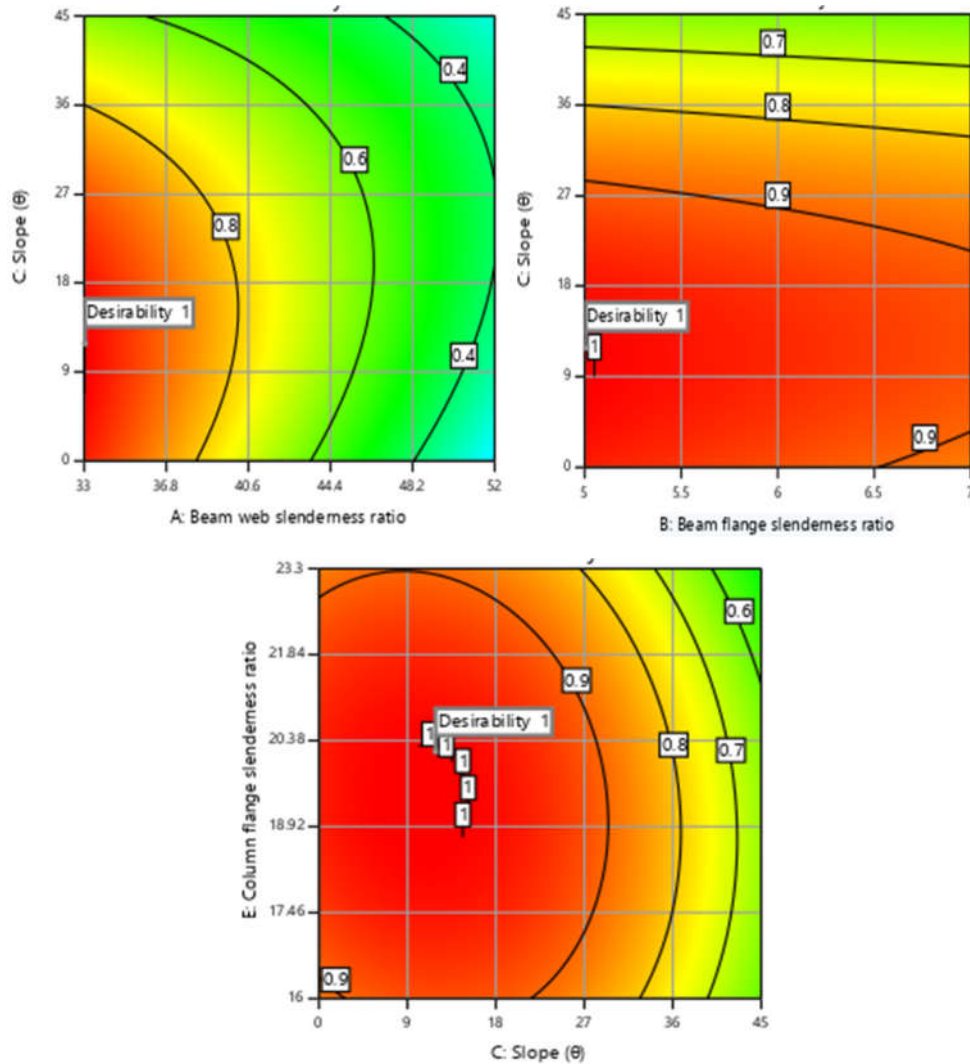


Figure 5.9. Contours plots of the desirability functions for different factors.

5.4.5 Results of the fifth optimization analysis

The fifth optimization analysis aimed at improving the structural response characteristics by only maximizing strength degradation rate (*SDR*). The optimum regions of the design space determined the best structural response characteristics where *SDR* is greater 1 which shows a low degradation rate. The optimal parameter achieved is are, beam web slenderness ratio = 33.34, beam flange slenderness ratio = 5.884, slope angle = 1.726°, RBS depth to beam flange width ratio = 0.113, column flange slenderness ratio = 19.705. The overall desirability function for this parameter combination is 1.

Figure 5.10 presents one-factor desirability plots at the optimal condition when desirability is 1. These plots illustrate the variation of desirability function changes with respect to each factor. For an optimal range for each factor where most desirable response are achieved; 80% of the maximum desirability will be used ($80\% \times 1 = 0.80$).

Figure 5.10(a) shows that lower beam web slenderness ratio is desirable for the maximizing strength degradation rate. The desirability function is decreased by increasing the beam web slenderness ratio from low level to high level. The optimal range for beam web slenderness ratio is from 33 to 40.

Beam flange slenderness ratio remained constant with a desirability of 100% with a slight change at about 6.1 which remained higher than 80% as shown in Figure 5.10(b)

Figure 5.10(c) suggests that maximum desirability was achieved between 0° and 1.7° , however a decrease in the desirability value was observed from 1.87° to 45° . The desirability range for beam slope angle ($D \geq 0.8$) is 0° to 20° .

From Figure 5.10(d) and 5.10(e), the desirability function is not sensitive to both RBS depth to beam flange width ratio column flange slenderness ratio and as desirability value above 80% was achieved through the entire range.

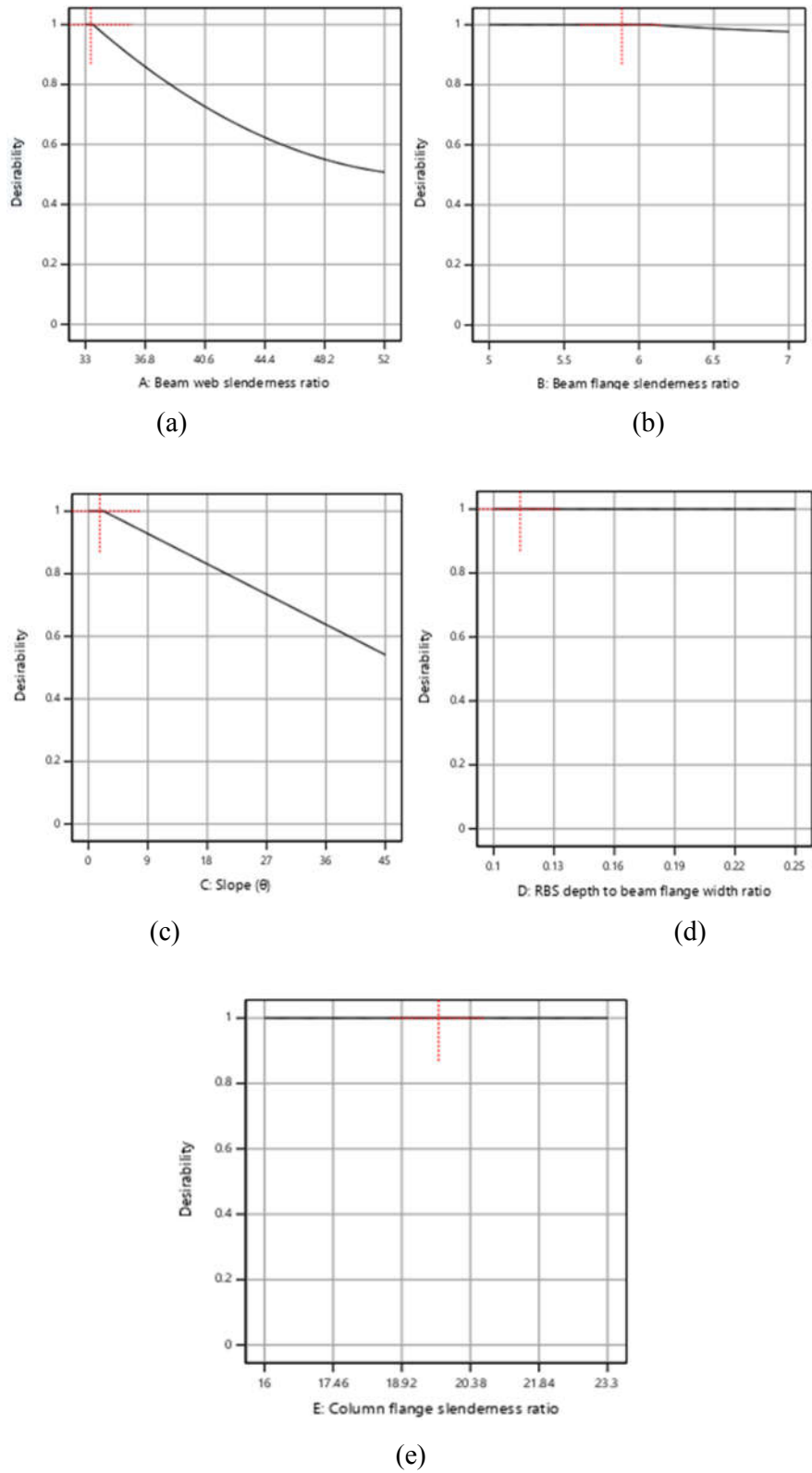


Figure 5.10. Fifth optimization analysis, the desirability function at the optimum condition versus: (a) beam web slenderness ratio; (b) beam flange slenderness ratio, (c) slope angle; (d) RBS depth to beam flange width ratio; (e) column flange slenderness ratio.

Figure 5.11. shows the contours plots of the desirability functions for different factors. The optimal conditions with desirability of 100%. The contours plot further support the optimization results illustrated above.

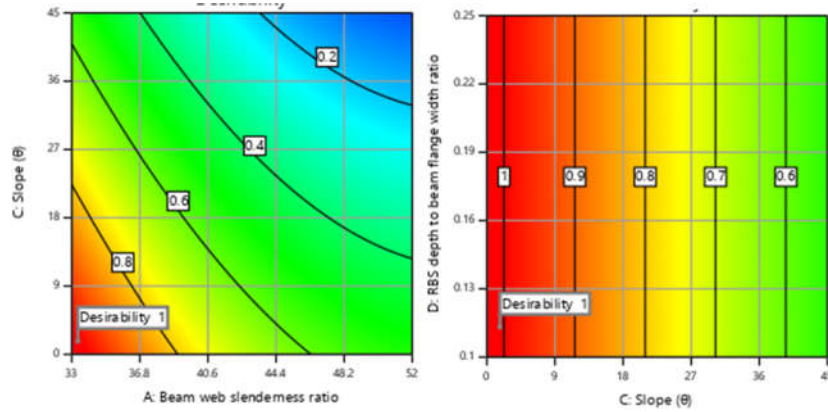


Figure 5.11. Contours plots of the desirability functions for different factors.

5.4.6 Results of the sixth optimization analysis

The sixth optimization analysis aimed at improving the structural response characteristics by minimising (*PI*) and maximizing strength degradation rate (*SDR*). The optimum regions of the design space determined the best structural response characteristics where low plastic strain index occur and *SDR* is greater 1 which shows a low degradation rate. The optimal parameter achieved is are, beam web slenderness ratio = 33.585, beam flange slenderness ratio = 5.231, slope angle = 0.312°, RBS depth to beam flange width ratio = 0.514, column flange slenderness ratio = 21.943. The overall desirability function for this parameter combination is 1.

Figure 5.12 presents one-factor desirability plots at the optimal condition when desirability is 1. These plots illustrate the variation of desirability function changes with respect to each factor. For an optimal range for each factor where most desirable response are achieved; 80% of the maximum desirability will be used ($80\% \times 1 = 0.80$).

Figure 5.12(a) shows that lower beam web slenderness ratio is desirable for the minimising plastic strain index (*PI*) and maximizing strength degradation rate. The desirability function is decreased by increasing the beam web slenderness ratio from low level to high level. The optimal range for beam web slenderness ratio is from 33 to 35.

Beam flange slenderness ratio remained constant with a desirability of 100% with a slight change at about 6.5 which remained higher than 80% as shown in Figure 5.12(b).

Figure 5.12(c) suggests that maximum desirability was achieved between 0° and 0.32°, however a decrease in the desirability value was observed from 0.32° to 45°. The desirability range for beam slope angle ($D \geq 0.8$) is 0 °to 24°.

Figure 5.12(d), RBS depth to beam flange width ratio remained constant with a desirability of 100% until a slight change at about 0.2 which remained higher than 80% as shown in figure Figure 5.12(e), the desirability function is not sensitive to column flange slenderness ratio and as desirability value above 80% was achieved through the entire range.

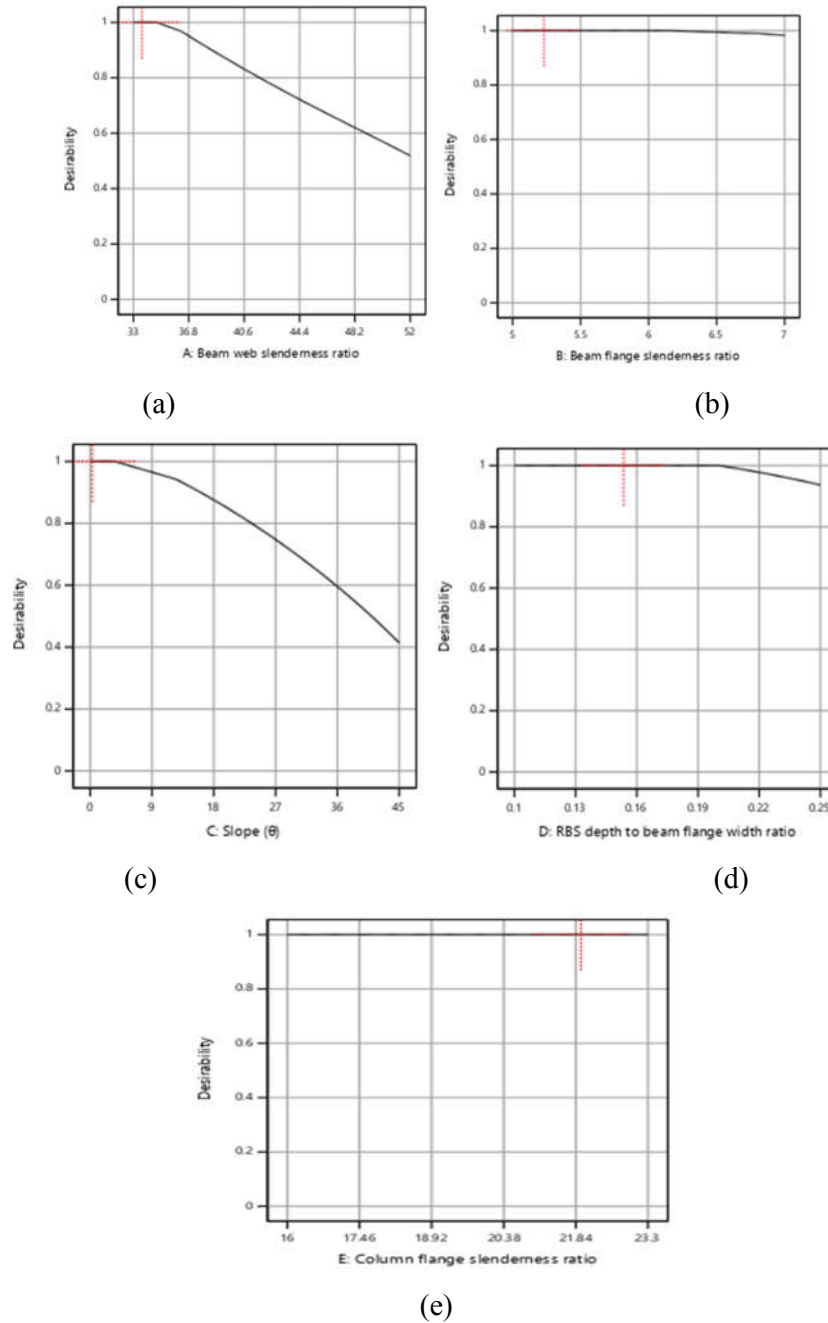


Figure 5.12. Sixth optimization analysis, the desirability function at the optimum condition versus: (a) beam web slenderness ratio; (b) beam flange slenderness ratio, (c) slope angle; (d) RBS depth to beam flange width ratio; (e) column flange slenderness ratio.

Figure 5.13. shows the contours plots of the desirability functions for different factors. The optimal conditions with desirability of 100%. The contours plot further support the optimization results illustrated above.

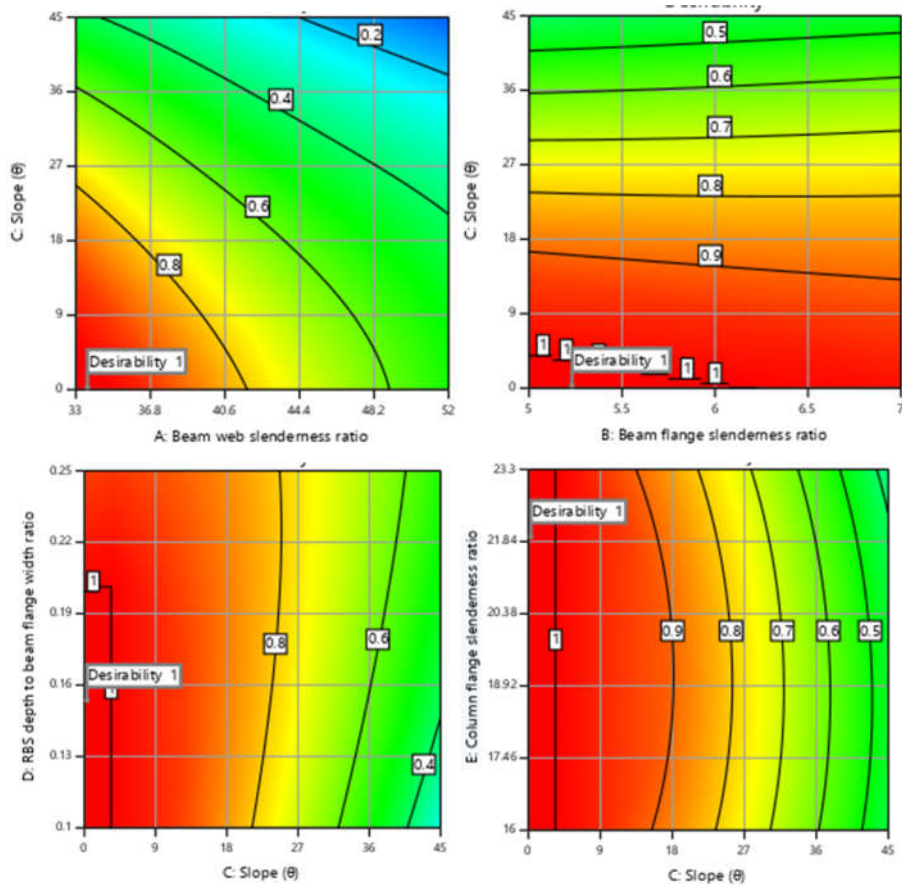


Figure 5.13. Contours plots of the desirability functions for different factors.

CHAPTER 6

6 SUMMARY AND CONCLUSION

6.1 Summary

The objective of this research aimed at generating predictive equations and optimizing the response characteristics of RBS moment connection. Using design of experiment and response surface methodologies, five important parameters were used to derive predictive equations for the response characteristics. Optimizations of the RBS moment connections were also achieved by minimising the local inelastic demand while maximizing all other response variables. For simultaneous optimization of multiple criteria of the responses, a desirability function approach was used. The results of the optimization study identified regions where greater desirability is achieved.

6.2 Conclusion

6.2.1 Predictive equations

Predictive equations were generated for responses such as Initial stiffness (K_i), Plastic strain index (PI), Moment capacity (M_{max}), Hysteretic energy dissipation (HED), and Strength degradation rate (SDR). 3D response plots were illustrated with the variation of each response with factors. The following conclusions are drawn from the study:

- Initial stiffness is increased by increasing the slope angle while other factors remained at the median value.
- Plastic strain index (PI) of RBS moment connection is increased with higher slope angle and beam web slenderness ratio. Smaller beam depth can be used to reduce the high inelastic demand
- Slope angle has a relatively higher influence on the moment capacity of the connection compared with the other significant factors. Therefore, increasing slope angle can increase moment capacity of the connection.
- Hysteretic energy dissipation increased with the slope angle and increased moment capacity.
- Increasing the slope angle and decreasing beam web slenderness ratio, low strength degradation rate can be achieved.
- For initial stiffness, plastic strain index, moment capacity, hysteretic energy dissipation, and strength degradation rate; R^2 values are 0.99, 0.98, 0.99, 0.99, and 0.83 respectively.

6.2.2 Optimization of sloped RBS connection

The results determined the optimal region of the input factors combination in which optimum conditions can be achieved. The optimal ranges for each factor are highlighted below:

- First optimization analysis indicated that having a slope angle higher than 27.82° , PI increases thereby fracture, and higher inelastic strain demand can occur. However, having low beam web slenderness ratio and larger beam flange slenderness ratio is beneficial in optimizing the response characteristics and minimising PI. The optimal parameters achieved are beam web slenderness ratio = 33, beam flange slenderness ratio = 7, slope angle = 27.82° , RBS depth to beam flange width ratio = 0.25, column flange slenderness ratio = 20.44. The overall desirability function for this parameter combination is 0.332.
- The results of the second optimization analysis indicated that low beam web slenderness ratio, low RBS depth to beam flange width ratio and larger beam flange slenderness ratio with beam slope at 21.52° is desirable for lower strength degradation rate. The optimal parameters achieved are beam web slenderness ratio = 33, beam flange slenderness ratio = 7, slope angle = 21.52° , RBS depth to beam flange width ratio = 0.11, column flange slenderness ratio = 23.3. The overall desirability function for this parameter combination is 0.26.
- Third optimization analysis showed that to minimise PI and maximise both HED and SDR, low beam web slenderness ratio, low beam flange slenderness ratio with beam slope angle ranging from (8° to 26°) is desirable. Although, it was observed that desirability reduces as slope angle is greater than 20° . The optimum regions of the design space determined the best structural response characteristics where higher strength degradation rate and low plastic strain index can be achieved. The optimal parameters achieved are beam web slenderness ratio = 33, beam flange slenderness ratio = 5, slope angle = 20° , RBS depth to beam flange width ratio = 0.176, column flange slenderness ratio = 19.2. The overall desirability function for this parameter combination is 0.634.
- Fourth optimization analysis indicated that to minimise PI only, the optimal parameter achieved is are, beam web slenderness ratio = 33.04, beam flange slenderness ratio = 5, slope angle = 11.87° , RBS depth to beam flange width ratio = 0.237, column flange slenderness ratio = 20.2. The overall desirability function for this parameter combination is 1. Thus, having low beam web slenderness ratio and beam flange

slenderness ratio with beam slope angle between (0° to 36°) is beneficial in minimizing *PI*. However, the maximum desirable for slope angle was achieved at 11.87° .

- The fifth optimization analysis aimed at improving the structural response characteristics by only maximizing strength degradation rate (*SDR*). It was observed that low beam web slenderness ratio and a slope of 1.7° is desirable to achieve *SDR* greater than 1. The optimal parameter achieved are, beam web slenderness ratio = 33.34, beam flange slenderness ratio = 5.884, slope angle = 1.726° , RBS depth to beam flange width ratio = 0.113, column flange slenderness ratio = 19.705.
- The sixth optimization analysis aimed at improving the structural response characteristics by minimising (*PI*) and maximizing strength degradation rate (*SDR*). It was observed that low beam web slenderness ratio and a slope of 0.312° is desirable to achieve low plastic strain index and *SDR* greater than 1. The optimal parameters achieved are, beam web slenderness ratio = 33.585, beam flange slenderness ratio = 5.231, slope angle = 0.312° , RBS depth to beam flange width ratio = 0.514, column flange slenderness ratio = 21.943.

Reduced beam section moment connections with beam slope angle is expected to possess higher initial stiffness in order to reduce lateral displacement which will control damage under minor to moderate earthquake. Also, having lower plasticity index and greater strength degradation rate can reduce the potential of fracture and occurrence of buckling in a frame structure. It can be concluded that RBS moment connection should have a low beam web slenderness ratio, high beam flange slenderness ratio with beam slope angle ranges from 11.87° to 27.82° . Beam slope angle greater than 27.8° will experience fracture, high inelastic demand with higher strength degradation and more intense buckling. Beam slope angle ranges between 11.9° to 27.8° will be the most effective in minimizing plasticity, having low strength degradation rate while maximizing initial stiffness, hysteresis energy dissipation and moment capacity.

APPENDICES

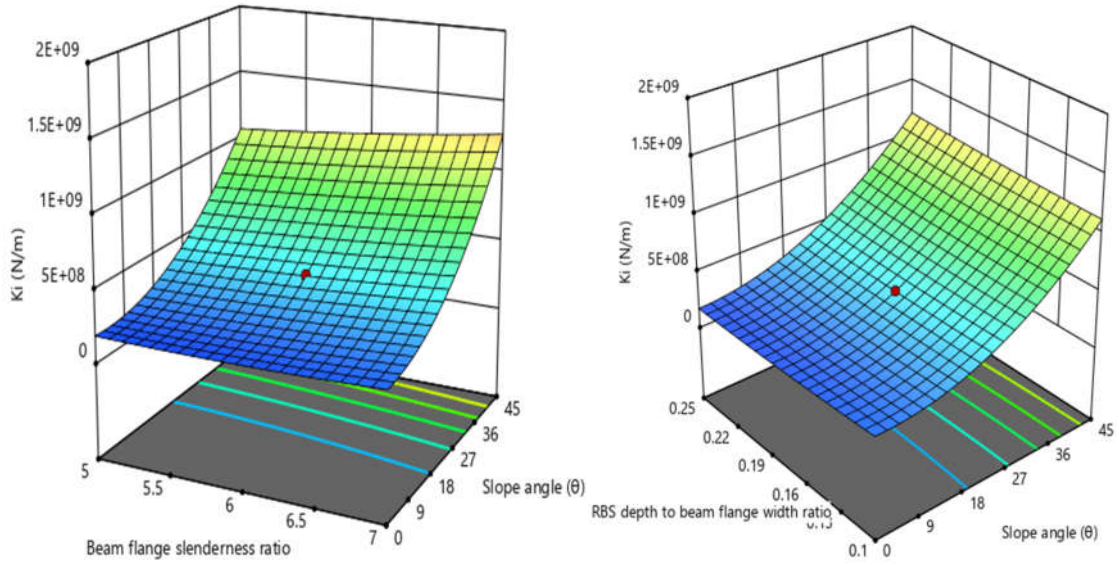


Figure A1. Variation of initial stiffness response variable to different factors

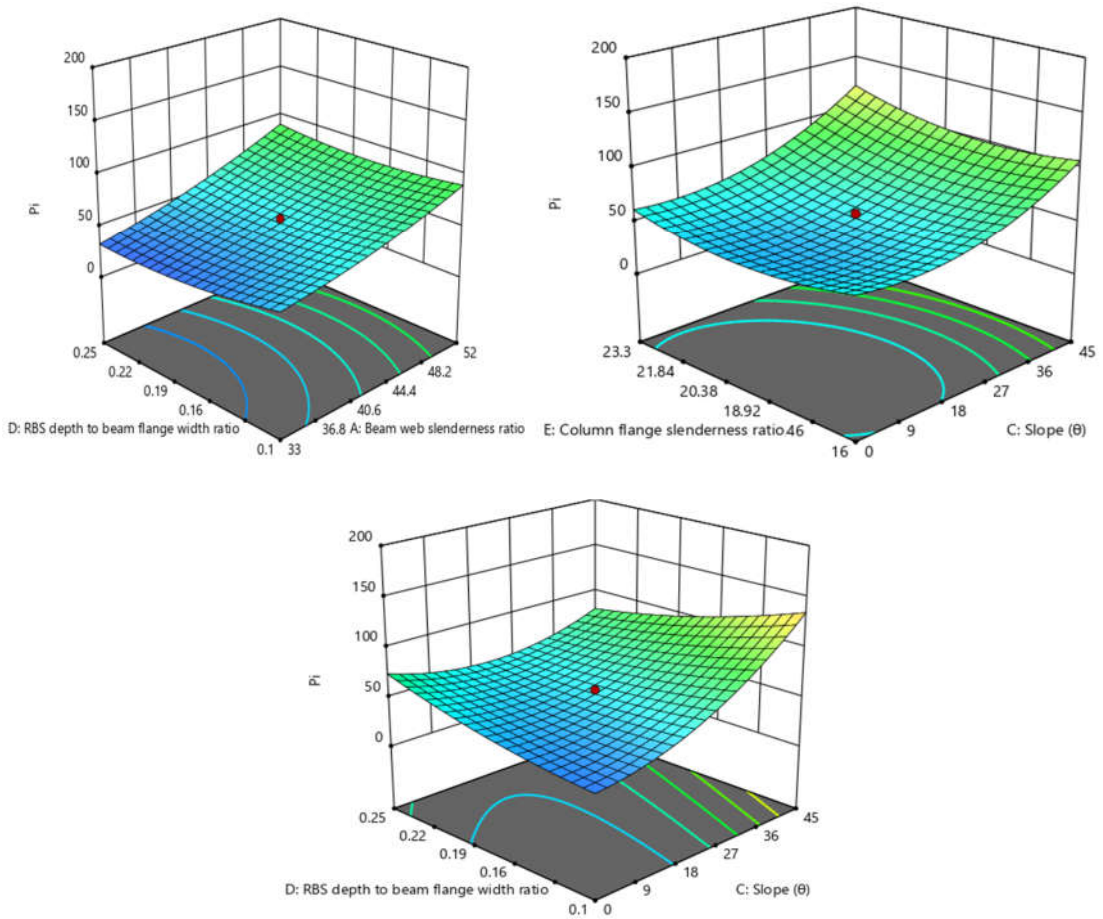


Figure A2. Variation of plastic strain index with respect to different factors

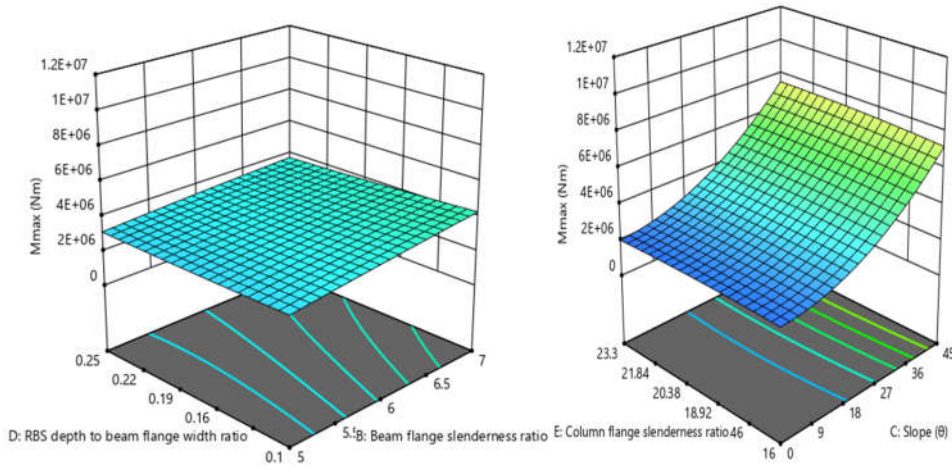


Figure A3. Variation of moment capacity with respect to different factors

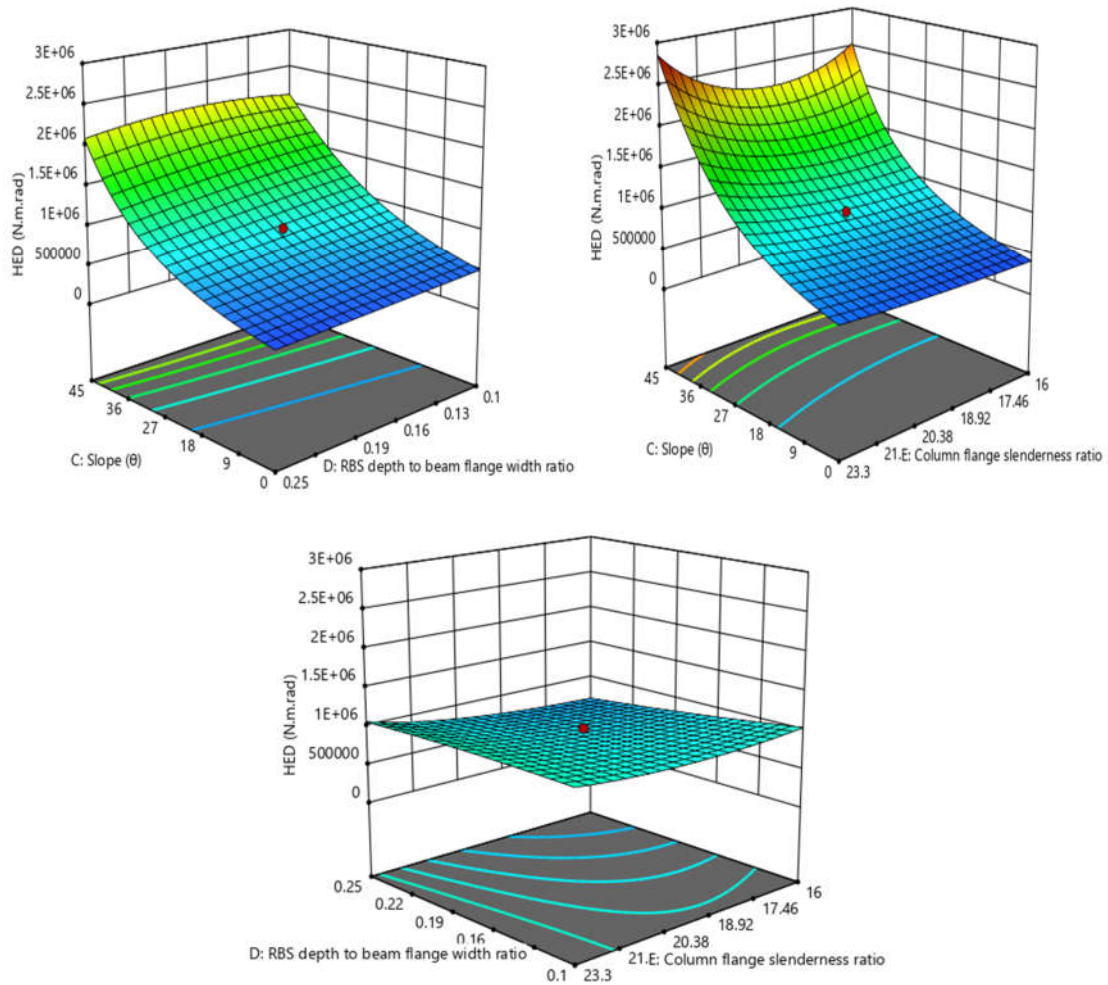


Figure A4. Variation of Hysteretic energy dissipation with respect to different factors

REFERENCES

- AISC, 2002. “*Seismic Provisions for Structural Steel Buildings*,” America Institute of steel construction, Chicago, Illinois.
- Ball, S. C. (2011). Steel non-orthogonal reduced beam section moment connections—a case study. *The Structural Design of Tall and Special Buildings*, 20, 14–29. <https://doi.org/10.1002/tal.737>
- Buratti, N., Ferracuti, B., & Savoia, M. (2010). Response Surface with random factors for seismic fragility of reinforced concrete frames. *Structural Safety*, 32(1), 42–51. <https://doi.org/10.1016/j.strusafe.2009.06.003>
- Derringer, G., & Suich, R. (1980). “Simultaneous optimization of several response variables.” *Journal of Quality Technology*, 12(4), 214–219.
- Desrochers, C., Prinz, G. S., & Richards, P. W. (2018). Column axial load effects on the performance of skewed SMF RBS connections. *Journal of Constructional Steel Research*, 150(Complete), 505–513. <https://doi.org/10.1016/j.jcsr.2018.09.007>
- DX12. (2019). “Design-Expert® Software Version 9.” Stat-Ease, Inc., Minneapolis, M.N.
- Ghassemieh, M., & Kiani, J. (2013). Seismic evaluation of reduced beam section frames considering connection flexibility. *The Structural Design of Tall and Special Buildings*, 622(16), 1248–1269. <https://doi.org/10.1002/tal.1003>
- Gilton Chad S., & Uang Chia-Ming. (2002). Cyclic Response and Design Recommendations of Weak-Axis Reduced Beam Section Moment Connections. *Journal of Structural Engineering*, 128(4), 452–463. [https://doi.org/10.1061/\(ASCE\)0733-9445\(2002\)128:4\(452\)](https://doi.org/10.1061/(ASCE)0733-9445(2002)128:4(452))
- Aswad H. N., Parung, H., Irmawaty, R., & Amiruddin, A. (2019). *Evaluation of reduced beam section (RBS) on castellated beam subjected to a seismic load* (Vol. 235). <https://doi.org/10.1088/1755-1315/235/1/012019>.
- Huh Jungwon & Haldar Achintya. (2001). Stochastic Finite-Element-Based Seismic Risk of Nonlinear Structures. *Journal of Structural Engineering*, 127(3), 323–329. [https://doi.org/10.1061/\(ASCE\)0733-9445\(2001\)127:3\(323\)](https://doi.org/10.1061/(ASCE)0733-9445(2001)127:3(323)).
- Hong, J. K. (2019). Sloped RBS Moment Connections at Roof Floor Subjected to Cyclic Loading: Analytical Investigation. *International Journal of Steel Structures*, 19(1), 329–339. <https://doi.org/10.1007/s13296-018-0198-4>
- Jin, J., & El-Tawil, S. (2005). Seismic performance of steel frames with reduced beam section connections. *Journal of Constructional Steel Research*, 61(4), 453–471. <https://doi.org/10.1016/j.jcsr.2004.10.006>

- Jones Scott L., Fry Gary T., & Engelhardt Michael D. (2002). Experimental Evaluation of Cyclically Loaded Reduced Beam Section Moment Connections. *Journal of Structural Engineering*, 128(4), 441–451. [https://doi.org/10.1061/\(ASCE\)0733-9445\(2002\)128:4\(441\)](https://doi.org/10.1061/(ASCE)0733-9445(2002)128:4(441))
- Kartal, M. E., Başıağa, H. B., & Bayraktar, A. (2011). Probabilistic nonlinear analysis of CFR dams by MCS using Response Surface Method. *Applied Mathematical Modelling*, 35(6), 2752–2770. <https://doi.org/10.1016/j.apm.2010.12.003>
- Kim Dong-Won, Ball Steven C., Sim Hyoung-Bo, & Uang Chia-Ming. (2016). Evaluation of Sloped RBS Moment Connections. *Journal of Structural Engineering*, 142(6), 04016013. [https://doi.org/10.1061/\(ASCE\)ST.1943-541X.0001459](https://doi.org/10.1061/(ASCE)ST.1943-541X.0001459).
- Lignos Dimitrios G., Kolios Dimitrios, & Miranda Eduardo. (2010). Fragility Assessment of Reduced Beam Section Moment Connections. *Journal of Structural Engineering*, 136(9), 1140–1150. [https://doi.org/10.1061/\(ASCE\)ST.1943-541X.0000214](https://doi.org/10.1061/(ASCE)ST.1943-541X.0000214)
- Moradi, S., & Mohammadi M.N. (2020). Effects of design factors on the cyclic response of sloped RBS moment connections. *Engineering structures (under review)*.
- Mashayekh, A. (2017). Sloped Connections and Connections with Fillet Welded Continuity Plates for Seismic Design of Special Moment Frames. *UC San Diego*. Retrieved from <https://escholarship.org/uc/item/7pw0c7sw>
- Micheal, D. Engelhardt (1999). T.R. Higgins Lecture: Design of Reduced Beam Section Moment Connection. Retrieved from <https://www.aisc.org/globalassets/aisc/awards/tr-higgins/past-winners/1999-t.r.-higgins-award-lecture--design-of-reduced-beam-section-moment-connections.pdf>
- Montgomery, D. C. (2013). *Design and analysis of experiments*. John Wiley & Sons, Inc.
- Moradi, S. (2016). Simulation, response sensitivity, and optimization of post-tensioned steel beam-column connections (T). University of British Columbia. Retrieved from <https://open.library.ubc.ca/cIRcle/collections/ubctheses/24/items/1.0228507>
- Moradi, S., & Burton, H. V. (2018). Response surface analysis and optimization of controlled rocking steel braced frames. *Bulletin of Earthquake Engineering*, 16(10), 4861–4892. <https://doi.org/10.1007/s10518-018-0373-1>
- Mohammad, A. H., Mahdi S. S., & Mohammad N. (2018). Response surface method for material uncertainty quantification of infrastructures. *Shock and Vibration*, vol. 2018, Article ID 1784203, 14 pages, 2018. <https://doi.org/10.1155/2018/1784203>.
- Ricles, M. J., & Zhang, X. (2006). *Seismic Performance of Reduced Beam Section Moment Connections to Deep Columns*. [https://doi.org/10.1061/40889\(201\)47](https://doi.org/10.1061/40889(201)47)

- Myers, R. H., Montgomery, D. C., & Anderson-Cook, C. M. (2016). *Response surface methodology: process and product optimization using designed experiments*. John Wiley & Sons.
- Oh, S.-H., Young-Ju, K., & Moon, T.-S. (2007). Cyclic performance of existing moment connections in steel retrofitted with a reduced beam section and bottom flange reinforcements. *Canadian Journal of Civil Engineering; Ottawa*, 34(2), 199–209.
- Ohsaki, M., Tagawa, H., & Pan, P. (2009). Shape optimization of reduced beam section under cyclic loads. *Journal of Constructional Steel Research*, 65(7), 1511–1519. <https://doi.org/10.1016/j.jcsr.2009.03.001>
- Plumier, A. New idea for safe structure in seismic zone. *Proceedings of IABSE Symposium on Mixed Structures Including New Materials.*, 431–436.
- Pachoumis, D. T., Galoussis, E. G., Kalfas, C. N., & Christitsas, A. D. (2009). Reduced beam section moment connections subjected to cyclic loading: Experimental analysis and FEM simulation. *Engineering Structures*, 31(1), 216–223. <https://doi.org/10.1016/j.engstruct.2008.08.007>
- Roudsari, M. T., Abdollahi, F., Salimi, H., Azizi, S., & Khosravi, A. R. (2015). The effect of stiffener on behavior of reduced beam section connections in steel moment-resisting frames. *International Journal of Steel Structures*, 15(4), 827–834. <https://doi.org/10.1007/s13296-015-1205-7>
- Sarkar, P., Ghosh, S., & Chakraborty, S. (2015). *AN EFFICIENT RESPONSES SURFACE METHOD FOR SEISMIC FRAGILITY ANALYSIS OF EXISTING BUILDING FRAME*.
- Seo, J., & Linzell, D. G. (2013). Use of response surface metamodels to generate system level fragilities for existing curved steel bridges. *Engineering Structures*, 52, 642–653. <https://doi.org/10.1016/j.engstruct.2013.03.023>
- Shahraki, H., & Shabakhty, N. (2015). Seismic Performance Reliability of RC Structures: Application of Response Surface Method and Systemic Approach. *Civil Engineering Infrastructures Journal*, 48(1), 47–68. <https://doi.org/10.7508/cej.2015.01.005>
- Simpson, T. W., Poplinski, J. D., Koch, P. N., & Allen, J. K. (2001). “Metamodels for computer-based engineering design: survey and recommendations.” *Engineering with Computers*, Springer, 17(2), 129–150.
- Towashiraporn, P., Duenas-Osorio, L., Craig, J. I., & Goodno, B. J. (2008). An application of the response surface metamodel in building seismic fragility estimation. *The World Conference on Earthquake Engineering, Beijing, China, Oct*, 12–17.
- Towashiraporn, P., Craig, J.I., & Goodno, B.J. (2002). Probabilistic response simulation and

regional vulnerability determination using response surface metamodels.

Zhao, Y.G., & Ono, T. (1998). System Reliability Evaluation of Ductile Frame Structures.

Journal of Structural Engineering, 124(6), 678–685.

[https://doi.org/10.1061/\(ASCE\)0733-9445\(1998\)124:6\(678\)](https://doi.org/10.1061/(ASCE)0733-9445(1998)124:6(678))